AD_____

Award Number: DAMD17-02-1-0136

TITLE: Regulatory Mechanism of EGFR-Mediated Oncogenic Signaling in Prostate Cancer Cells

PRINCIPAL INVESTIGATOR: Jiing-Dwan Lee, Ph.D.

CONTRACTING ORGANIZATION: The Scripps Research Institute
La Jolla, California 92037

REPORT DATE: February 2004

TYPE OF REPORT: Final

PREPARED FOR: U.S. Army Medical Research and Materiel Command
Fort Detrick, Maryland 21702-5012

DISTRIBUTION STATEMENT: Approved for Public Release;
Distribution Unlimited

REPORT DOCUMENTATION PAGE

Form Approved
OMB No. 074-0188

1. AGENCY USE ONLY (Leave blank)	2. REPORT DATE	3. REPORT TYPE AND DATES COVERED
	February 2004	Final (15 Jan 2002 - 15 Jan 2004)

4. TITLE AND SUBTITLE
Regulatory Mechanism of EGFR-Mediated Oncogenic Signaling in Prostate Cancer Cells

5. FUNDING NUMBERS
DAMD17-02-1-0136

6. AUTHOR(S)
Jiing-Dwan Lee, Ph.D.

7. PERFORMING ORGANIZATION NAME(S) AND ADDRESS(ES)
The Scripps Research Institute
La Jolla, California 92037

E-Mail: grants@scripps.edu

8. PERFORMING ORGANIZATION REPORT NUMBER

9. SPONSORING / MONITORING AGENCY NAME(S) AND ADDRESS(ES)
U.S. Army Medical Research and Materiel Command
Fort Detrick, Maryland 21702-5012

10. SPONSORING / MONITORING AGENCY REPORT NUMBER

11. SUPPLEMENTARY NOTES

12a. DISTRIBUTION / AVAILABILITY STATEMENT
Approved for Public Release; Distribution Unlimited

12b. DISTRIBUTION CODE

13. ABSTRACT (Maximum 200 Words)

The EGFR receptor tyrosine kinase is dysfunctional in a wide range of solid human tumors including prostate carcinomas. The EGFR gene product is a transmembrane glycoprotein belonging to the epidermal growth factor receptor family and its cytoplasmic domain is responsible for sending the mitogenic signals into cells. We discovered that this domain of EGFR interacts with Tid1 protein, a human counterpart of Drosophila tumor suppressor Tid56. Tid56 null mutation causes lethal tumorigenesis during larvae stage. Tid1 is also known as a chochaperone of the heat shock protein 70 (Hsp70) and binds to Hsp70 through its conserved DnaJ-domain. We found that increased expression of Tid1 in human carcinoma attenuates the EGFR-dependent oncogenic ERK1/2 and BMK1 signaling pathways. Importantly, the functional DnaJ-domain of Tid1 is required for consequent suppression of oncogenic signaling of carcinoma cells resulting from increased Tid1 expression. Together, these results suggest that Tid1 deterring uncontrolled proliferation of carcinoma cells through reducing the downregulating the cancerous signaling from EGFR. Moreover, the cochaperonic and regulatory function of Tid1 on Hsp70 most likely play an essential role of this anti-proliferation function of Tid1 in carcinoma cells.

14. SUBJECT TERMS
No Subject Terms Provided.

15. NUMBER OF PAGES
24

16. PRICE CODE

17. SECURITY CLASSIFICATION OF REPORT	18. SECURITY CLASSIFICATION OF THIS PAGE	19. SECURITY CLASSIFICATION OF ABSTRACT	20. LIMITATION OF ABSTRACT
Unclassified	Unclassified	Unclassified	Unlimited

Table of Contents

Introduction:

This grant was originally proposed for three years but was reduced to two years during reviewing processes. Therefore, this 2nd year report is considered to be the final report of this grant.

The goal of this proposal is to improve our knowledge of the signaling deregulation of ErbB receptor, which contributes to the malignancy of prostate cancer. Specifically, we will examine the function and the mechanism of action of an ErbB-interacting protein Tid1. The Drosophila *l(2)tid* gene, *Tid56*, is the first and only member of the DnaJ cochaperone family that has been classified as a tumor suppressor. The null mutation of the *Tid56* gene not only keeps imaginal discs from differentiation but also leads to lethal tumorigenesis during the larvae stage, suggesting that during embryogenesis *Tid56* is involved in regulating cell differentiation, cell growth, and cell death. The function of its mammalian counterpart, *Tid1*, in animals and in cells, however, has not been fully characterized. DnaJ proteins serve as cochaperones and regulatory factors for the Hsp70 family of molecular chaperones, and are characterized by a J domain, a highly conserved tetrahelical domain that binds to Hsp70s to regulate their activity and provide substrate specificity. In fact, it has been shown that Tid1 interacts with Hsp70s residing in cytosol (Hsp70/Hsc70) or in mitochondria (mtHsp70) through its DnaJ domain, indicating that Tid1 might exert its cellular function by modulating the activity and substrate-binding specificity of these Hsp70s. It is hoped that the proposed research will help developing novel strategies to control the malignant properties of prostate cancer.

Body:

Task1:

For Task 1, we have proposed to study the role of Tid1 in ErbB-dependent cellular signaling in human cancer cells. In Task 1.1, we proposed to study the scope of the inhibitory effect of Tid1 on EGFR-dependent intracellular signal transduction. To test this, we infected LNCaP cells with recombinant adenovirus encoding Tdi1S or control virus and later transferred into serum-free medium for 24hrs followed by EGF stimulation for 15 min (Figure 1). Activation of MAP kinses BMK1 by EGF in these treated cells was analyzed using migration retardation using antiBMK1 antibody. The EGF-dependent activation of p38, JNK and PI-3K pathways were examined by anti-phospho p38, JNK and Akt antibodies respectively by Western Blotting (Figure 1). On the other hand, the c-Src activity in these treated cells was analyzed by in vitro kinase assay using exogenous enolase as substrate (Figure 1). We found that the increased Tid1 expression significantly reduced the activation of the mitogenic BMK1 pathway by the induction of EGF in prostate cancer cells. However, the EGF-dependent activation of PI-3K pathway in prostate cancer cells was not affected by the elevated intracellular Tid1 protein. On the other hand, in LNCap cells, the activities of p38, JNK and c-Src were not significantly changed by the treatment of EGF (Figure 1), and the increased Tid1 does not affect the basal activity of these signaling pathways. Together, we concluded that Tid1 has profound inhibitory effect on EGF-induced BMK1 activation but not PI-3K, Src, p38 and JNK pathways.

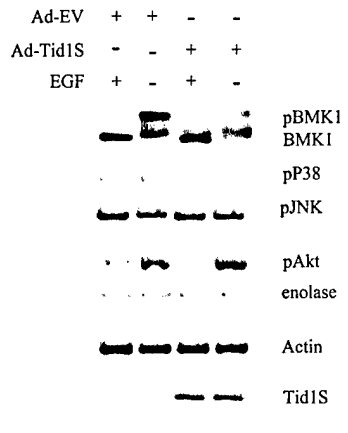

Figure 1. Increased expression of Tid1S influences the EGFR-mediated intracellular signaling. LNCaP cells were infected with recombinant adenovirus encoding Tid1S or control virus as indicated. The following day the infected cells were transferred into serum-free medium for 24 hr and then stimulated with 1ng/ml EGF for 15 min. Whole cell lysates from these cells were subjected to Western blot analysis. The first panel shows the EGF-induced activation of downstream BMK1/ERK5 using an anti-BMK1 antibody (NEB). The second panel shows the level of endogenous phospho-p38 using anti-phospho p38 antibody. The third panel shows the level of endogenous phospho-JNK using anti-phospho JNK antibody. The fourth panel shows the level of endogenous phospho-Akt using anti-phospho Akt antibody. The fifth panel shows the activity of endogenous Src kinase using enolase as substrate in an in vitro kinase assays. The sixth panel shows the level of endogenous actin using anti-actin antibody to demonstrate equal loading. The bottom panel shows the expression of endogenous and recombinant Tid1S using the anti-Tid1 antibody.

For Task1.2, we proposed to examine the biological effect of Tid1on the malignant properties of prostate cancer cells. We have generated recombinant adenovirus encoding wt Tid1 and Tid1 mutants carrying either point mutation or deletion mutation. To assess the function of Tid1 in human prostate cancer line, LNCaP was infected with recombinant adenovirus encoding Tid1 and its mutants Tid1(HQ) and Tid1 (CT). Typical apoptotic morphology characterized by loss of adherence, condensed cytoplasm, and

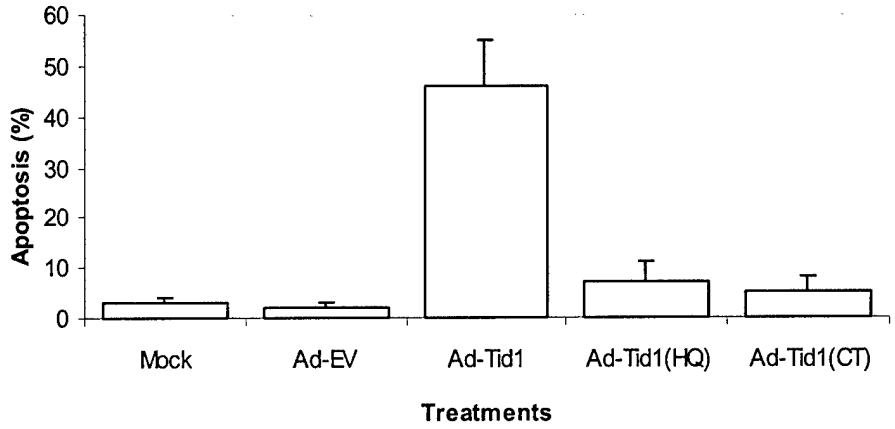

Figure 2. Increased cellular Tid1 led to apoptosis of prostate cancer cells and the DnaJ and c-terminal domain of Tid1 is vital for this Tid1-mediated PCD. LNCaP cells were infected with Ad-Tid1 (column 3) or its mutants as indicated (Columns 4 and 5). Columns 1 and 2 represent cells infected with nothing or the empty vector (Ad-EV). Cells were mock infected or infected with control virus (Ad-EV), Ad-Tid1s or Ad-Tid1 mutants as indicated, fixed and followed by TUNEL assay after 3 days. TUNEL positive cells were counted as apoptotic cells. % Apoptosis = TUNEL positive cell number/ total cell number.

formation of apoptotic bodies in dying cells were observed in the light microscopy at 6 days post-infection with Ad-Tid1s (Figure 2). Similar results were also found in the cells infected with Ad-Tid1$_L$ indicating Tid1L has similar apoptosis-inducing effect on carcinoma cells as Tid1S (data not shown). The percentage of cell underwent program

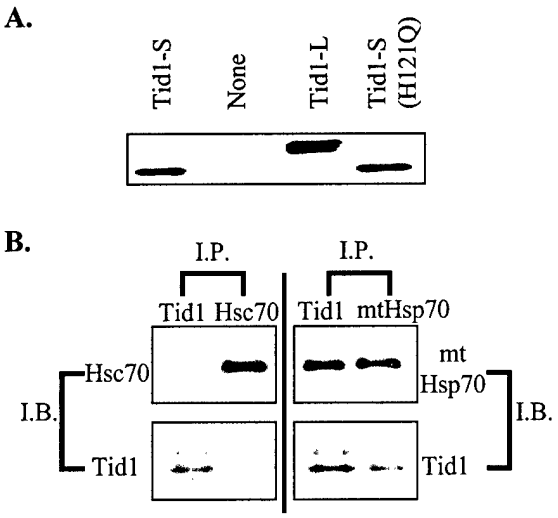

Fig. 3. Endogenous Tid1_L and Tid1-S proteins coimmunoprecipitated with Hsp 70. (*A*) Total proteins were collected from *Tid1*$^{f/-}$ MEFs infected with recombinant adenoviruses encoding human Tid1-L, Tid1-S, or Tid1-S (H121Q) as indicated and analyzed by Western blotting with the anti-Tid1 antibody. (*B*) Endogenous Tid1-L and Tid1-S proteins coimmunoprecipitated with mtHsp70. Total protein from MEF cells was used for immunoprecipitation experiments with antibodies specific for Tid1, mtHsp70, or Hsc70. The resulting immunocomplexes were analyzed by immunoblotting with antibodies against Tid1, mtHsp70, or Hsc70, as indicated.

cell death were quantified by TUNEL assay (Figure 2). Approximately 45% of the cancer cells were apoptotic by increased expression of Tid1 whereas apoptotic bodies were only 1-7% in those cells infected with adenoviruses encoding control (AD-EV) or mutant Tid1 [Tid1(HQ) and Tid1(CT)]. Interestingly, none of hTid1s mutants, including the J domain mutant (HQ), C-terminal deletion mutant (CT) (Figure 2) induced apoptosis. These data suggest that both DNA J domain (critical for the binding of Tid1 to Hsp 70) and C-terminus of Tid1 (responsible for its interaction with ErbB) (Figure 2) are required for Tid1-mediated carcinoma apoptosis.

To further investigate how Tid1 exert its anti-tumor function in carcinoma cells, we further examine its other cellular targets. The Tid1 protein has been shown to interact with both mitochondria heat shock protein 70 (mtHsp70) and non-mitochondria Hsp70. Nonetheless, Syken *et al.* reported that in human osteosarcoma cells, U2OS, the Tid1 protein interacts only with mtHsp70 but not with cytosolic Hsp70 (Hsc70). To identify with which Hsp70 Tid1 interacts in MEFs, we used specific antibodies against Tid1, mtHsp70, or the non-mitochondrial Hsp70 homolog, Hsc70, in coimmunoprecipitation-immunoblot experiments. The antibody specific for mouse Tid1 immunoprecipitated both mature forms of Tid1 associated with mtHsp70, but did not immunoprecipitate Hsc70 from cells (Figure 3). The antibody specific for mtHsp70 protein immunoprecipitated mtHsp70 in complex with Tid1, but in immunoprecipitates prepared from cell extracts with the anti-Hsc70 antibody, no Tid1 was detected (Figure 3). We further investigated the subcellular localization of Tid1 in cells by immunofluorescence microscopy. In *Tid1*$^{f/+}$ cells, 5 days after Ad-Cre infection, endogenous Tid1 and mtHsp70 were separately stained by using antibodies specific for either Tid1 or mtHsp70. Both Tid1 and mtHsp70 were detected mostly in the cytoplasm, colocalized, and displayed a short filamentous pattern (Figure 4*A*). Not surprisingly, no Tid1 protein could be detected in Ad-Cre treated *Tid1*$^{f/-}$ cells, and interestingly, the subcellular distribution of mtHsp70

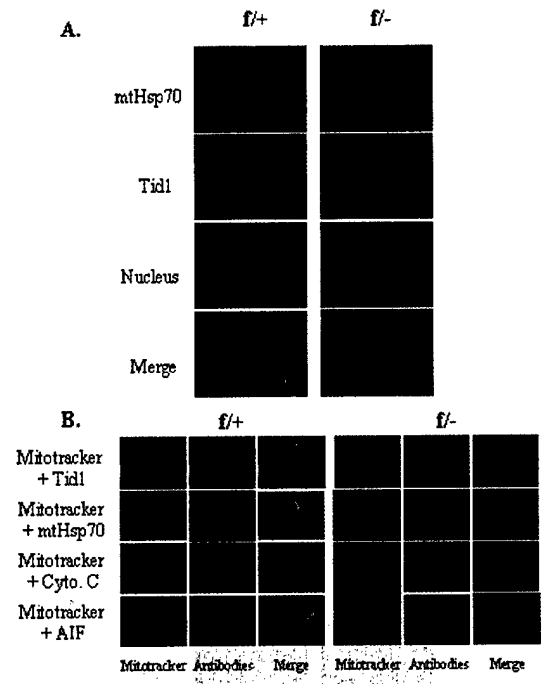

Fig. 4. Tid1 and mtHsp70 proteins colocalize within mitochondria. (*A*) Immunofluorescence staining of Tid1 and mtHsp70 protein in *Tid1*$^{f/+}$ and *Tid1*$^{f/-}$ MEF cells 5 days after treatment with Ad-Cre. (*B*) Same Ad-Cre treated *Tid1*$^{f/+}$ and *Tid1*$^{f/-}$ MEF cells were first stained with Mitotracker and subsequently double stained with antibodies against Tid1, mtHsp70, cytochrome c or AIF as indicated.

turned punctate (Figure 4*A*). The change of the subcellular distribution of mtHsp70 from short filament to punctate was not dependent on the genotype of cells, since before deletion of *Tid1*, mtHsp70 and Tid1 colocalized in a short-string pattern within the cytosol of *Tid1*$^{f/-}$ cells (data not shown). These data suggest that Tid1 protein in cells is located within cytoplasm and that mtHsp70 is the major Hsp70 in complex with Tid1. To further examine the subcellular localization of Tid1 or mtHsp70 in MEFs, Mitotracker, a mitochondrial specific dye, was used. In *Tid1*$^{f/+}$ cells 5 days after Ad-Cre infection, most of the Tid1 co-stained with the Mitotracker demonstrating that Tid1 proteins were mainly restricted within the mitochondria (Figure 4*B*). Similar patterns were observed when *Tid1*$^{f/+}$ cells were double-stained with Mitotracker and mtHsp70, Mitotracker and cytochrome c or Mitotracker and AIF (apoptosis-inducing factor) (Figure 4*B*). In Ad-Cre treated *Tid1*$^{f/-}$ cells, the intensity of Mitotracker staining was attenuated compared to that of *Tid1*$^{f/+}$ cells (Figure 4*B*). Interestingly, some AIF proteins were translocated from mitochondria to nucleus suggesting that the Tid1-deleted *Tid1*$^{f/-}$ cells were undergoing the process of cell death (Figure 4*B*).

In Task 1.3, we proposed to identify the tyrosine residue(s) in the Tid1, which is phosphorylated after EGF induction. We expressed Tid1 deletion mutants (described in Figure 6) in LNCaP cells followed by EGF induction and Western blot analysis as described in legend of Figure 5, we found that tyrosine phosphorylation of Tid1 is located in the C-terminal of Tid1 (aa292-aa 453). Since there are five tyrosine residues (aa 369, aa 399, aa 401, aa 405 and aa 427) exist in this region, we constructed five Tid1 mutants

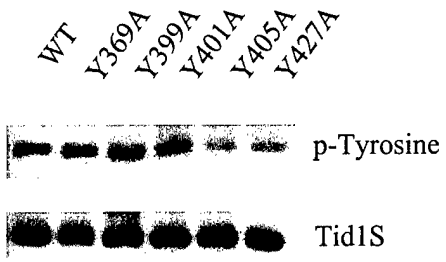

Figure 5. Tyrosine phosphorylation of Tid1 mutants in prostate cancer cells. LNCaP cells were transfected with mutant constructs as indicated and later transferred into serum-free medium for 24 hr and then stimulated with 1ng/ml EGF for 15 min. Anti-Tid1 antibody was used to immunoprecipiate these Tid1 mutant in cell lysates from these cells as indicated at the top of the figure. Western blots were performed on corresponding cell lysates using anti-phosphotyrosine antibody 4G10 (Upstate Biotechnology) to detect the tyrosine phosphorylation of Tid1 (top panel). The anti-Tid1 antibody (described in the preliminary data section) was used to verify the immunoprecipitation of Tid1 mutants (bottom panel).

by mutating each of these tyrosines individually to alanines as indicated in figure 5. These mutants together with wildtype constructs were transfected into LNCaP cells separately, and later these cells were transferred into serum-free media for 24 hours. These treated cells were stimulated with 1 ng/ml EGF for 15 min, total cell lysates were prepared from these cells, and Tid1 mutants were immunoprecipitated and separated in SDS/PAGE gel. The level of tyrosine phosphorylation in these proteins was analyzed in Western blot suing anti-phospotyrosine antibody as described in legend of Figure 5. We found that the level of tyrosine phosphorylation was significantly reduced only in mutants Y405A and Y427A but not in the rest of mutants indicating that the tyrosine residues 405 and 427 but not the tyrosine residues 369, 399 and 401 in Tid1 were phosphorylated in prostate cancer cells after EGF induction.

Task 2:

For Task 2, we have proposed to study the structural basis for the role of Tid1 in ErbB-mediated signaling. In Task2.1 and 2.2, we proposed to identify the structural domains in Tid1S or EGFR cytoplasmic domain required for the interaction of Tid1 and EGFR. For this, we have generated Tid1 and EGFR mutants with different motifs deleted or with key amino acids mutated as well as generated recombinant adenoviruses of some of these mutants. In addition, we have generated polycolonal antibodies against various domains of Tid1 to facilitate this Task. The plasmids encoding wt EGFR and individual Tid1 mutant were contranfected into 293 T cell followed by immunoprecipation using anti-Tid1 antibodies, and immunobloting the immunoprecipitates with anti-EGFR antibody. We found that the C-terminal region of Tid1 (a.a. 293-453) is required and sufficient for Tid1 interaction with the signaling domain of EGFR (Figure 6). On the other hand, for Task 2.2, we have constructed yeast expressing vectors encoding fusion protein containing GAL4-BD domain fused with various portions of cytoplasmic domain of EGFR as indicated (Figure 7). These mutants were individually transformed into the yeast stain PJ69-2 together with a yeast-expressing vector encoding fusion protein containing GAL4-AD domain fused with Tid1. Transformed yeasts were cultured on plates containing the indicated selective media (Figure 7). The growth of these tranformed yeasts in the selective media is dependent on the interaction between individual EGFR mutants and Tid1 in each yeast two-hybrid based assays. From these assays, we discovered that the C-terminal region of

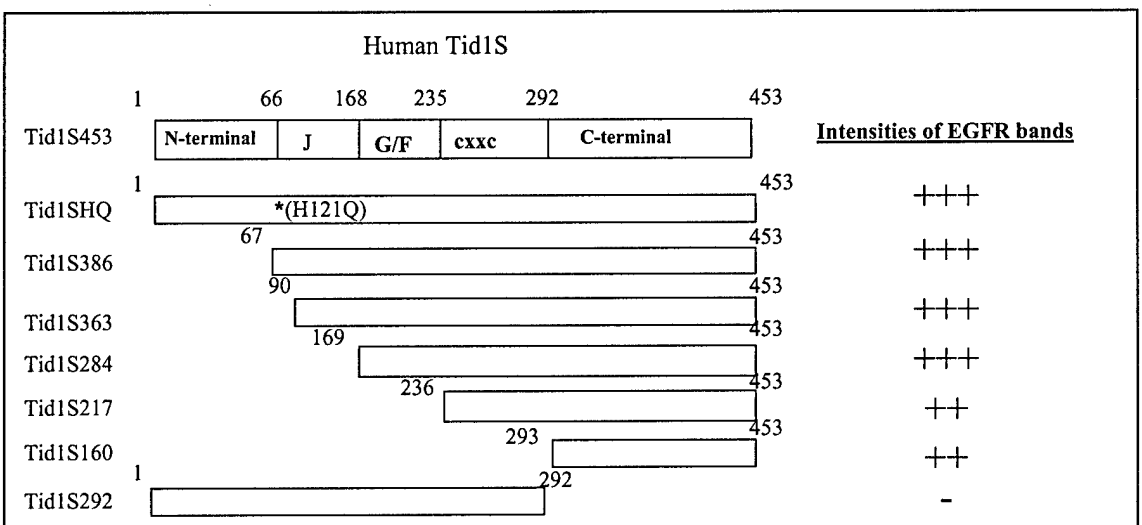

Figure 6. The C-terminus (a.a. 293-453) of Tid1S is required and sufficient for interaction between Tid1S and the cytoplamic portion of EGFR in coimmunoprecipitation..

We constructed mammalian expression plasmids that expressing a wildtype or portions of Tid1S as indicated. 293T cell was cotransfected with these plasmids individually with vestor encoding human EGFR. After 48 hrs, cells were lysed, immunoprecipiated with anti-Tid1 anbody followed by immunobloting with anti-EGFR antibody. The intensities of EGFR bands were quantititated by desitometer and shown in the right panel.

EGFR signaling domain between amino acid 1150 and 1186 but not the region between amino acid 644 and 1150 is critical for the interaction between Tid1 and the cytoplasmic domain of EGFR (Figure 7). Next, to further elucidate the cellular role of Tid1 in mammalian cells, we deleted Tid1 gene in MEFs using Cre/lox dependent mechanism followed by cDNA microarray. We examined 13,000 known genes to determine the gene expression profiles altered by *Tid1* removal. Total RNA from both Ad-Cre infected $Tid1^{f/+}$ and $Tid1^{f/-}$ MEFs was purified and examined by cDNA microarray-based analysis. After statistical analysis, we found a total of 91 genes that showed a greater than 2-fold change caused by disrupting both Tid1 alleles. Among these, we found that the expression of the BAG1 and MEK7 genes, important for cell growth and survival, decreased more than 2.5-fold in cells without the Tid1 protein. Semiquantitative reverse transcription-polymerase chain reaction (RT-PCR) analysis was used to confirm the results from the cDNA microarray (Fig 8*A*). Additionally, by immunoblot assay, the decreased expression of BAG1 and MEK7 proteins after *Tid1* deletion was established by comparing their expression levels in $Tid1^{f/+}$ and $Tid1^{f/-}$ MEFs after Ad-Cre treatment. The expression of the internal control, β-actin, was not altered in these two treated MEFs (Fig. 8*B*).

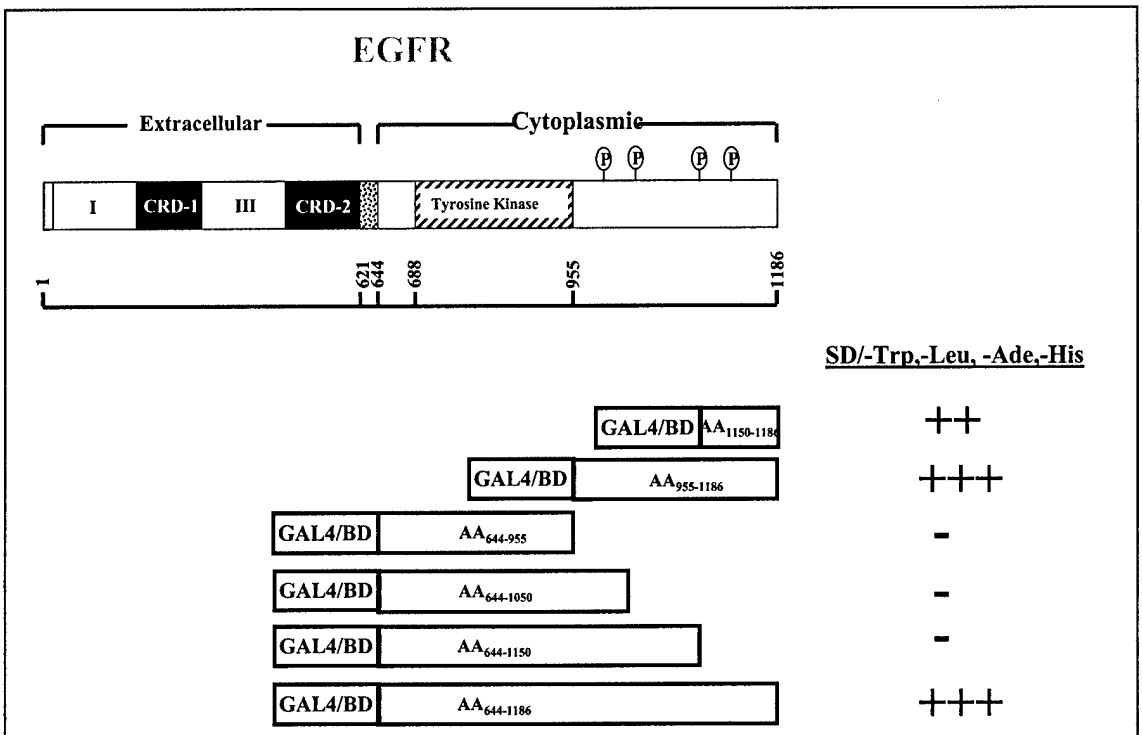

Figure 7. Indentifying domain of EGFR interacting with Tid1. We constructed yeast expression vectors encode fusions between GAL4 binding domain and portions of the EGFR intracellular domain as indicated. The yeast strain PJ69-2A was cotransfomred with vectors encoding BD/EGFR(mutants) along with the AD/Tid1 fusion protein as indicated. Transformed yeast was cultured on plates containing the indicated selective media, and the growth rates of these yeasts are shown on the right.

Key research accomplishment:

1st year:

- We have generated mutants of Tid1 with point mutations in its conserved J-domain and deletion mutants in several conserved leader sequence, DNA J, G/F and CXXX as well as C-terminal non-conserved domains.
- We have produced recombinant adenoviruses for the abovementioned Tid1 mutants and tested for their effectiveness in infecting and expressing these mutants in human cancer cells.
- We have developed siRNA vectors that can specifically reduce the expression level of cellular Tid1.
- We have generated polyclonal antibodies specifically against different portions of Tid1 protein.
- We have examined the selective intracellular pathways for the effect of increased expression of Tid1 in cancer cells and found that BMK1 pathway but not JNK, p38, PI-3K and c-Src pathways are affected by increased Tid1 in prostate cancer cells.

2nd year:

- We discovered that C-terminus (aa292-aa453) of Tid1s is required and sufficient for the interaction of Tid1 with EGFR.
- We found that the intracellular region of EGFR between aa 1150-aa1186 is required for the binding of Tid1.
- We have identified tyrosine residues of Tid1 that are phosphorylated after EGF stimulation in prostate cancer cells.
- We found that Hsp70 protein of human carcinoma cells exists in the immunocomplexes derived from anti-Tid1.
- Our data indicate that the inhibition of cell proliferation caused by increased Tid1 expression is most likely the result of cell death.
- Our results indicate that increased Tid1 in human carcinoma cells leads to apoptosis, and Tid1 domains required for EGFR- (C-terminal) or Hsp70-binding (J domain) are both critically involved in this Tid1-mediated PCD of cancer cells.
- Our results indicate that removing endogenous Tid1 leads to the decreased expression of BAG1 and MEK7 partially in mammalian cells (1).
- We produced the Tid1-floxed (*Tid1$^{f/f}$*) mice, which developed to adulthood normally and appeared to be healthy for at least 12 months after birth (1).

Reportable outcomes:

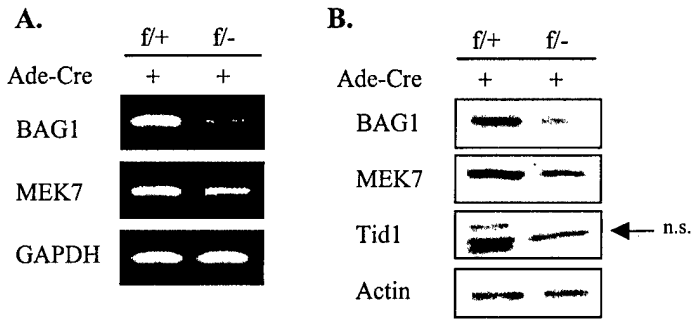

Fig. 8. Decreased expression of *BAG1* and *MEK7* genes caused by cellular Tid1 removal. (*A*) *Tid1$^{f/+}$* and *Tid1$^{f/-}$* MEF cells were infected with Ad-Cre, and after 6 days, total RNAs from these MEF cells were collected and analyzed by semi-quantitative RT-PCR with the specific primer sets for *BAG1*, *MEK7*, or *GAPDH*. The PCR products were separated through 4% agarose. (*B*) Total cellular extracts were prepared from these Ad-Cre–treated *Tid1$^{f/+}$* and *Tid1$^{f/-}$* cells and analyzed by immunoblotting with anti-Tid1, anti-BAG1, anti-MEK7, or anti β-actin antibodies as indicated. n.s., non-specific.

Using the high efficient transducing adenovirus vectors encoding different forms of Tid1 and Tid1 mutant proteins, we have discovered that the C-terminal motif of Tid1 is required and sufficient for the physical binding of Tid1 and the signal transduction domain of EGFR. Interestingly, in addition to EGFR, Tid1 also complexes with cellular Hsp70 protein which could be important for the downregulation of signaling capacity of EGFR in prostate carcinoma cells and also for the apoptosis of human prostate carcinoma cells. In order to study the role of Tid1 in a organismal

context during prostate tumor progression, we have produced a Tid1-floxed mouse model and this animal appeared to be normal. This model will be later crossed with prostate cancer model to examine the outcome of Tid1 deletion in prostate tumorigenesis. We have also found that the endogenous Tid1 is involved in regulating the expression of signaling molecules MEK7 and BAG1, which may contribute to the anti-tumor function of Tid1.

Conclusions:

EGFR/ErbB1 is a receptor tyrosine kinase that heterodimerizes with other members of the ErbB family. Its active cytoplasmic domain provides docking sites for various signaling molecules that link ErbB activation to numerous intracellular signaling pathways that lead to a variety of cell responses, including proliferation, differentiation, survival, and apoptosis. Deregulation of ErbB-dependent signaling network by ErbB malfunction is involved in the development of malignancy of numerous types of human cancers. Therefore, identifying molecules that interact with the intracellular domain of EGFR will contribute not only to the elucidation of the regulatory mechanism of ErbBs in cancer progression but also to the development of new treatments for uncontrolled growth of human cancers. To this end, by using the cytoplasmic region of EGFR as bait in yeast two-hybrid screening, we discovered that the signaling domain of EGFR interacts with Tid1 protein, which is the human counterpart of Drosophila tumor suppressor Tid56. Tid56 null mutation causes tumorous imaginal discs resulting from continuous cell proliferation without differentiation. To date, the mechanism of tumor suppression of Tid56 in *Drosophila*, as well as the cellular function of Tid1 in human tumorigenesis, are poorly understood. After confirming that Tid1 interacts with EGFR in mammalian cells, we found that increasing the expression of this protein in prostate cancer cells has a potent inhibitory effect on intracellular oncogenic signaling and on the subsequent proliferation of cancer cells. These results suggest that Tid1 attenuates signals generated from the EGF receptor and, like its *Drosophila* counterpart, may be an important tumor suppressor, especially in prostate cancer.

References:

1. Jeng-Fan Lo, Masaaki Hayashi, Sung Woo Kim, Bin Tian, Jing-Feng Huang, Colleen Fearns, Shin Takayama, Juan M. Zapata, Young Yang and Jiing-Dwan Lee. Tid1, a cochaperone of the heat shock 70 protein and the mammalian counterpart of the Drosophila tumor suppressor l(2)tid, is critical for early embryonic development and cell survival. 2004. Molecular and cellular Biology. In Press.

Appendices:

1. Lo, J.-F., Hayashi, M., Kim. S.W., Tian, B. Huang, J.-F., Fearns, C., Takayama, S., Zapata, J.M., Yang, Y., and Lee, J.-D. Tid1, a cochaperone of the heat shock 70 protein and the mammalian counterpart of the Drosphila tumor supressor 1(2)tid, is critical for early embryonic development and cell survival. 2004. Molecular and Cellular Biology. 24:2226-2236.

MOLECULAR AND CELLULAR BIOLOGY, Mar. 2004, p. 2226–2236 Vol. 24, No. 6
0270-7306/04/$08.00+0 DOI: 10.1128/MCB.24.6.2226–2236.2004

Tid1, a Cochaperone of the Heat Shock 70 Protein and the Mammalian Counterpart of the *Drosophila* Tumor Suppressor l(2)tid, Is Critical for Early Embryonic Development and Cell Survival

Jeng-Fan Lo,[1] Masaaki Hayashi,[1] Sung Woo-Kim,[1] Bin Tian,[2] Jing-Feng Huang,[3] Colleen Fearns,[1] Shinichi Takayama,[4] Juan M. Zapata,[4] Young Yang,[3] and Jiing-Dwan Lee[1]*

Department of Immunology, The Scripps Research Institute,[1] and The Burnham Institute,[4] La Jolla, California 92037; University of Medicine and Dentistry of New Jersey-New Jersey Medical School, Newark, New Jersey 07103[2]; and Johnson and Johnson Pharmaceutical Research and Development, San Diego, California 92121[3]

Received 1 August 2003/Returned for modification 7 October 2003/Accepted 3 December 2003

Tid1 is the mammalian counterpart of the *Drosophila* tumor suppressor Tid56 and is also a DnaJ protein containing a conserved J domain through which it interacts with the heat shock protein 70 (Hsp70) family of chaperone proteins. We generated a Tid1 conditional mutation in mice, and the subsequent global removal of the Tid1 protein was achieved by crossing these conditional knockout mice with general deletor mice. No *Tid1*$^{-/-}$ embryos were detected as early as embryonic day 7.5 (E7.5). Nonetheless, Tid1-deficient blastocysts were viable, hatched, formed an inner cell mass and trophectoderm, and implanted (E4.5), suggesting that the homozygous mutant embryos die between E4.5 and E7.5. To assess the function of Tid1 in embryonic cells, mouse embryonic fibroblasts with the homologous *Tid1* floxed allele were produced. Tid1 removal in these cells led to massive cell death. The death of Tid1-deficient cells could be rescued by ectopic expression of wild-type Tid1 but not by expression of the Tid1 protein that had a mutated J domain and was thus incapable of binding to Hsp70. We propose that Tid1 is critical for early mammalian development, most likely for its function in sustaining embryonic-cell survival, which requires its association with Hsp70.

The *Drosophila l(2)tid* gene, *Tid56*, encodes the first and only member of the DnaJ cochaperone family that has been classified as a tumor suppressor (16, 17). The null mutation of the *Tid56* gene not only keeps imaginal disks from differentiation but also leads to lethal tumorigenesis during the larval stage, suggesting that during embryogenesis *Tid56* is involved in regulating cell differentiation, cell growth, and cell death (16, 17). The function of its mammalian counterpart, *Tid1*, in animals and in cells, however, has not been fully characterized. DnaJ proteins serve as cochaperones and regulatory factors for the heat shock protein 70 (Hsp70) family of molecular chaperones (24) and are characterized by a J domain, a highly conserved tetrahelical domain that binds to Hsp70 proteins to regulate their activities and provide substrate specificity (24). In fact, it has been shown that Tid1 interacts with Hsp70 proteins residing in cytosol (Hsp70/Hsc70) or in mitochondria (mtHsp70) through its DnaJ domain, indicating that Tid1 might exert its cellular function by modulating the activities and substrate-binding specificities of these Hsp70 proteins (25, 27).

Tid1 was originally isolated by yeast two-hybrid screening as a protein that interacts with the human papillomavirus E7 oncoprotein (22). Several reports have indicated that Tid1 functions as a regulator in intracellular signaling pathways related to cell survival, cell proliferation, and stress-induced cellular responses. For example, in agonist-induced programmed cell death, Tid1 has a role in both apoptotic and antiapoptotic processes (25). Tid1 has also been suggested to regulate intracellular signaling through its affinity with the RasGAP protein to modulate the Ras signaling pathway (27) and through its binding to Jak2 to regulate gamma interferon-dependent transcriptional activity (21). Additionally, it has been observed that Tid1 associates with human T-cell leukemia virus type 1 Tax and subsequently, by inhibiting IKKβ kinase activity, represses NF-κB activation induced by Tax, tumor necrosis factor alpha, and Bcl10 (6, 7).

To date, most information regarding the function of Tid1 has been generated from cell-based assays. To examine the function of Tid1 in vivo, we generated a conditional knockout mouse model of Tid1 and subsequently elucidated the role of Tid1 during early embryogenesis.

MATERIALS AND METHODS

Genomic DNA cloning of mouse Tid1. Mouse genomic DNA containing the *Tid1* gene was isolated by PCR-based screening of a bacterial artificial chromosome library derived from 129/SvJ mouse embryonic stem (ES) cells (Incyte, St. Louis, Mo.). The primer sets used for screening were designed based on the mouse *Tid1* sequence (GenBank accession no. AC079418): Tid99355U21 (5′-TGTCCCCGGGCCAAAATGGCT-3′) and Tid99562L21 (5′-TGGTGTTCCCCACGCTGGTTG-3′), and Tid94263U21 (5′-CCGCAGGAAGCAAGGATAGGC-3′) and Tid95069L21 (5′-CTCGGCGGTTCAGAGGGATCT-3′).

Disruption of the *Tid1* gene in ES cells. A deletion allele of *Tid1* was generated by introducing a double-stranded DNA linker, *Sal*I-FRT-loxP-*Xho*I, into the *Xho*I site of the pPNT vector (28). The following PCR products from three regions were subcloned separately and later inserted into the modified pPNT vector: a 2.7-kb product of 5′-untranslated sequence, exon 1, and partial intron 1; a 0.8-kb product with partial intron 1, exon 2, and part of intron 2; and a 2.8-kb product containing partial intron 2, exon 3, and partial intron 3 (Fig. 1A). One extra loxP site was introduced by synthetic oligonucleotides in the middle of intron 1, and the second frt site was inserted into intron 2 as indicated in Fig. 1A. In the final targeting construct, the neomycin resistance (Neo) cassette of pPNT was flanked by two frt sites, and the exon 2-containing fragment of the *Tid1* gene (0.8 kb) was flanked by two loxP sites. The orientation of the transcribed Neo

* Corresponding author. Mailing address: Department of Immunology, The Scripps Research Institute, 10550 N. Torrey Pines Rd., La Jolla, CA 92037. Phone: (858) 784-8703. Fax: (858) 784-8343. E-mail: jdlee@scripps.edu.

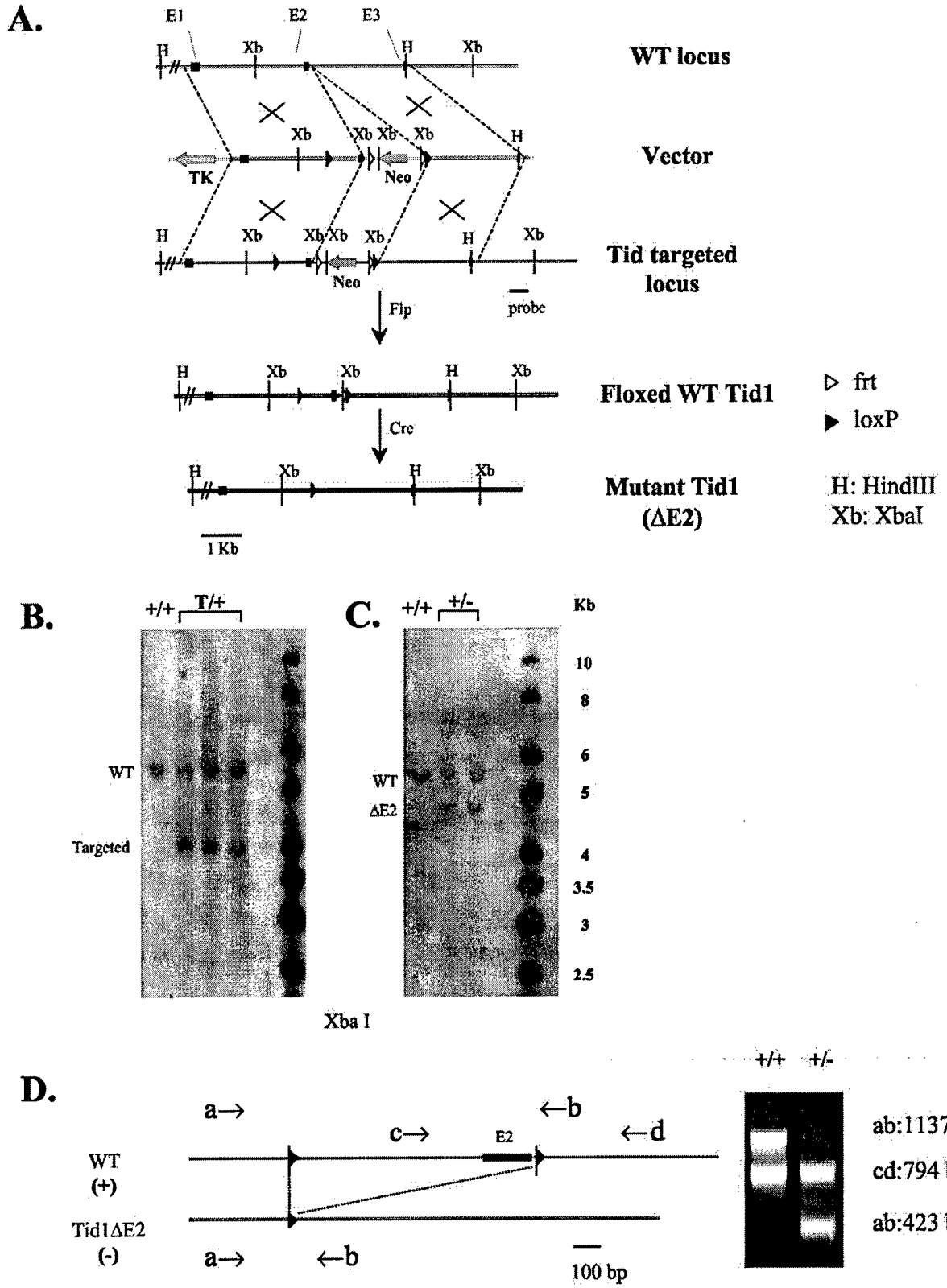

FIG. 1. Targeted disruption of the mouse *Tid1* gene. (A) Partial restriction maps of the *Tid1* locus, targeting vector, targeted locus, and targeted locus after Cre-mediated *Tid1* deletion. The first three exons are indicated by solid boxes. WT, wild type; TK, thymidine kinase. (B) Genotyping ES cell clones by Southern blot hybridization of genomic DNA (restriction digestion with *Xba*I enzyme) with the probe shown in panel A. The genotype of each clone is indicated. T, targeted. (C) Genotyping mice derived from the cross between Tid1-targeted mice and general deletor mice by Southern blot analysis as described for panel B. (D) Genotyping $Tid1^{+/+}$ and $Tid1^{+/-}$ mice by PCR. The PCR primers used for genotyping are indicated by arrows and are depicted along with maps of the corresponding alleles. On the right are the patterns of electrophoresed PCR products for $Tid1^{+/+}$ and $Tid1^{+/-}$ mice.

cassette was in the opposite direction to that of *Tid1*. The insertion, orientation, and sequence fidelity of the inserted DNA fragments within the targeting vector were confirmed by DNA sequencing. Further details are available upon request.

The *Not*I-linearized targeting vector was introduced by electroporation into ES cells derived from the 129/SvJ mouse strain (Incyte, St. Louis, Mo.). Colonies resistant to 200 μg of G418 (GIBCO-BRL, Carlsbad, Calif.)/ml and 1 μM ganciclovir (Calbiochem, San Diego, Calif.) were picked and screened for homologous recombination first by PCR with the upstream Neo-specific primer Tidpcrp9997U30 (5′-CCAGTCCCTTCCCGCTTCAGTGACAACGTC-3′) and the downstream Tid1-specific primer Tidpcrp14009L30 (5′-TCCCGAGATCAG CTATCAATATGAATTACC-3′). Individual ES clones that passed the first screen were cultured and analyzed by Southern blotting and DNA sequencing in a second screen for clones containing two intact loxP sites flanking exon 2 of the *Tid1* gene (*Tid1* floxed) (Fig. 1B). Three clones of ES cells contained the targeting vector with the desired genomic integration site that had been introduced via homologous recombination.

Generation of *Tid1* mutant and floxed mice. Three clones of targeted ES cells were injected separately into C57BL/6 blastocysts and later implanted into C57BL/6 pseudopregnant females (Jackson Laboratories, Bar Harbor, Maine). One highly chimeric male was produced and backcrossed to C57BL/6 females. The offspring were genotyped by Southern blotting and PCR analyses (details below) to detect germ line transmission from the chimeric male (Fig. 1B). To delete the Neo cassette in the $Tid1^{+/targeted}$ mice for generating mice with a functional *Tid1* floxed allele, $Tid1^{+/targeted}$ mice were crossed with transgenic B6/J-TgN(ACTFLPe) mice (Jackson Laboratories) carrying an ACTB-FLPe gene (Fig. 1A and data not shown). Deletion of the *Tid1* gene in *Tid1* floxed mice was achieved by crossing $Tid1^{+/targeted}$ mice with transgenic FVB/N-TgN(ACTB-Cre) mice (Jackson Laboratories) carrying the ACTB-Cre gene (Fig. 1A, C, and D). The resulting $Tid1^{+/-}$ mice were maintained in a 129/SvJ, C57BL/6, and FVB/N mixed background and were later intercrossed to generate $Tid1^{-/-}$ embryos for subsequent studies. All animal protocols were in full compliance with the guidelines for animal care and were approved by the Animal Care Committee of the Scripps Research Institute.

Southern and PCR analyses for genotyping. For genotyping ES cell lines to identify targeted clones, 10 μg of genomic DNA was digested with *Xba*I, separated by electrophoresis through 0.7% agarose in 1× TAE buffer, blotted onto a nylon membrane (Nytran SuPerCharge; Schleicher & Schuell, Keene, N.H.), and probed with a 0.5-kb PCR fragment (Fig. 1A) that hybridizes downstream of the targeted region of *Tid1*. The 5.6-kb band corresponds to the wild-type allele, and the 4.0-kb band corresponds to the targeted allele (Fig. 1B). For genotyping weaned pups, genomic DNA was purified from tail biopsy specimens and analyzed by either Southern blotting or PCR analysis. For Southern analysis, 10 or 20 μg of DNA was digested with *Xba*I, separated by electrophoresis, blotted, and probed with the PCR product described above (Fig. 1A). The 5.6-kb fragment corresponds to the wild-type allele, and the 4.8-kb fragment corresponds to the mutant allele (ΔExon2) (Fig. 1C). For PCR analysis, genomic DNA was used as the template in a reaction where wild-type and mutant alleles were detected simultaneously. Four primers were designed to differentiate between the presence of wild-type and mutant *Tid1* alleles. Primer a (5′-TCTAATGTCTTC TCCGGGAGT-3′), primer b (5′-AGTGACCAGACCAGCAATCTT-3′), and primer d (5′-TTTCCCAAAAGACCTGAACTC-3′) hybridized to both wild-type and *Tid1*/ΔExon2 alleles. Primer c (5′-GAATCAAATTCAGGGCCTTGT-3′) hybridized to the wild-type allele only and did not hybridize to the *Tid1*/ΔExon2 allele (Fig. 1D). Primers a and b amplified a 1,137-bp fragment from the wild-type allele and a 423-bp fragment from the *Tid1*/ΔExon2 allele (Fig. 1D). Primers c and d amplified a 794-bp fragment from the wild-type allele but did not amplify any product from the *Tid1*/ΔExon2 allele (Fig. 1D).

Embryos at different embryonic stages were genotyped by PCR analysis of DNA purified from either the yolk sac or the whole embryo. Tissues were digested overnight at 55°C in 300 μl of lysis buffer (50 mM Tris-HCl, pH 8.0–100 mM EDTA–0.5% sodium dodecyl sulfate [SDS]–500 μg of proteinase K/ml). DNA was purified by phenol-chloroform extraction, precipitated with isopropanol, and dissolved in 100 μl of 50 mM Tris-HCl (pH 8.0). This purified DNA (2 μl) was used for PCR-based genotyping as described above.

Blastocysts and blastocyst outgrowths were genotyped by nested PCR. The outgrowths were washed once with phosphate-buffered saline (PBS). Then, either blastocysts or outgrowths were lysed in 20 μl of PCR lysis buffer (10 mM Tris-HCl, pH 8.3–50 mM KCl–2.5 mM $MgCl_2$–0.1 μg of gelatin/ml–0.45% NP-40–0.45% Tween 20–500 μg of proteinase K/ml) at 55°C for 1 h and then at 95°C for 10 min. Purified DNA (2 μl) was later used in the first PCR amplification with primers e (5′-CCAAGTATCGAGGTCTAATGT-3′) and f (5′-TCAGCTACA GTGTACCCCTAT-3′), which are located upstream and downstream from primers a and d, respectively, and a PCR product of ~2 kb was generated (data not shown). The PCR conditions were the same as described above, except that the annealing temperature was 60°C instead of 55°C. This PCR product (2 μl) served as the template in a subsequent PCR amplification with primer sets ab and cd.

TABLE 1. Genotypes of progeny from heterozygous matings[a]

Stage	No. with genotype			No. of empty implantations
	+/+	+/−	−/−	
At weaning	41	80	0	
E13.5	10	17	0	7
E12.5	7	9	0	5
E10.5	18	34	0	19
E9.5	3	6	0	2
E8.5	5	18	0	10
E7.5	5	12	0	9
Blastocysts	14	26	9	

[a] Genotypes were determined by PCR.

Timed pregnancies. For monitoring timed pregnancies, 6- to 10-week-old $Tid1^{+/-}$ females were mated with $Tid1^{+/-}$ males. The females were examined each morning for the presence of a vaginal plug (14). The females were sacrificed at E7.5, E8.5, E9.5, E10.5, E12.5, or E13.5 to isolate embryos. The isolated embryos were genotyped by PCR as described above.

Isolation of E3.5 embryos and in vitro culturing. Three- to 9-week-old $Tid1^{+/-}$ females were superovulated by injection intraperitoneally with pregnant mare's serum gonadotropin (5 IU per animal; Sigma-Aldrich Co. or Professional Compounding Centers of America, Houston, Tex.), followed by injection with 5 IU of human chorionic gonadotropin (Sigma-Aldrich Co. or Serono Laboratories, Randolph, Mass.), and 48 h later were mated with $Tid1^{+/-}$ males (18). At E3.5, the treated females were sacrificed, and embryos were isolated from their oviducts and cultured for 3 days in ES medium. For blastocyst outgrowth, individual blastocysts were placed on gelatin-coated 96-well plates with 0.2 ml of ES cell medium supplemented with leukemia inhibitory factor and were cultured again for 3 days (18). Outgrowths were photographed, washed with PBS, and lysed for genotyping by PCR as described above.

Antibody generation and immunoblot analysis. Antiserum against mouse Tid1 was generated in a New Zealand White rabbit (Animal Center of The Scripps Research Institute, La Jolla, Calif.) by using the synthetic oligopeptide (IQT DQKIRLTGKGIPRINC) derived from the mouse Tid1 amino acid sequence. The anti-MEK7 antibody was purchased from Santa Cruz Biotechnology (Santa Cruz, Calif.). For immunoblots, cells were lysed for 10 min on ice in 50 mM Tris-HCl (pH 7.5), 10 mM EDTA, 1% SDS, 1 mM dithiothreitol, 2 mM phenylmethylsulfonyl fluoride, 15 μg of aprotinin/ml, and 2 μg of pepstatin/ml. Protein lysates were cleared by centrifugation for 20 min at 16,000 × *g* and 4°C, and protein concentrations were measured by the Bradford assay (Bio-Rad, Hercules, Calif.). Cell lysates (10 to 30 μg) were fractionated by SDS-polyacrylamide gel electrophoresis, and the proteins were transferred to nitrocellulose membranes (Bio-Rad). The membranes were blocked for 10 min in blocking buffer (10 mM Tris-HCl, pH 8.0–50 mM NaCl–0.2% Tween 20–5% nonfat dry milk), incubated with primary antibody for 2 h in blocking buffer (with 0.5% nonfat milk), and incubated in blocking buffer with horseradish peroxidase-conjugated anti-rabbit immunoglobulin G (IgG; Pierce Biotechnology, Rockford, Ill.).

Generation of MEFs (14). Mouse embryonic fibroblasts (MEFs) with the genotypes $Tid1^{+/+}$, $Tid1^{+/-}$, $Tid1^{fl/-}$, $Tid1^{fl/+}$, and $Tid1^{fl/fl}$ were generated by crossing $Tid1^{fl/+}$ mice with $Tid1^{fl/+}$ or $Tid1^{+/-}$ mice, and the resulting E13.5 embryos were collected. The yolk sac of each embryo was isolated and used for genotyping. Individual embryos were minced and then treated with trypsin for 10 min. After being washed with Dulbecco's modified Eagle's medium (DMEM) containing 15% fetal bovine serum, the MEFs were cultured in DMEM supplemented with 15% fetal bovine serum on 12-well plates coated with 0.1% gelatin.

Construction, preparation, and infection of recombinant adenovirus. The AdEasy vector system from Qbiogene, Inc. (Carlsbad, Calif.), was used according to the manufacturer's protocol to generate recombinant adenoviruses encoding human Tid1-L, Tid1-S, Tid1-S (H121Q), MEK7, or BAG1. Recombinant adenovirus encoding Cre recombinase under the control of the cytomegalovirus immediate-early promoter (Ad-Cre) was a gift from Shuang Huang, The Scripps Research Institute (La Jolla, Calif.). 293 cells were cultured in DMEM containing 10% fetal calf serum and used for producing recombinant adenoviruses. High-titer stocks of individual adenovirus particles were prepared by equilibrium

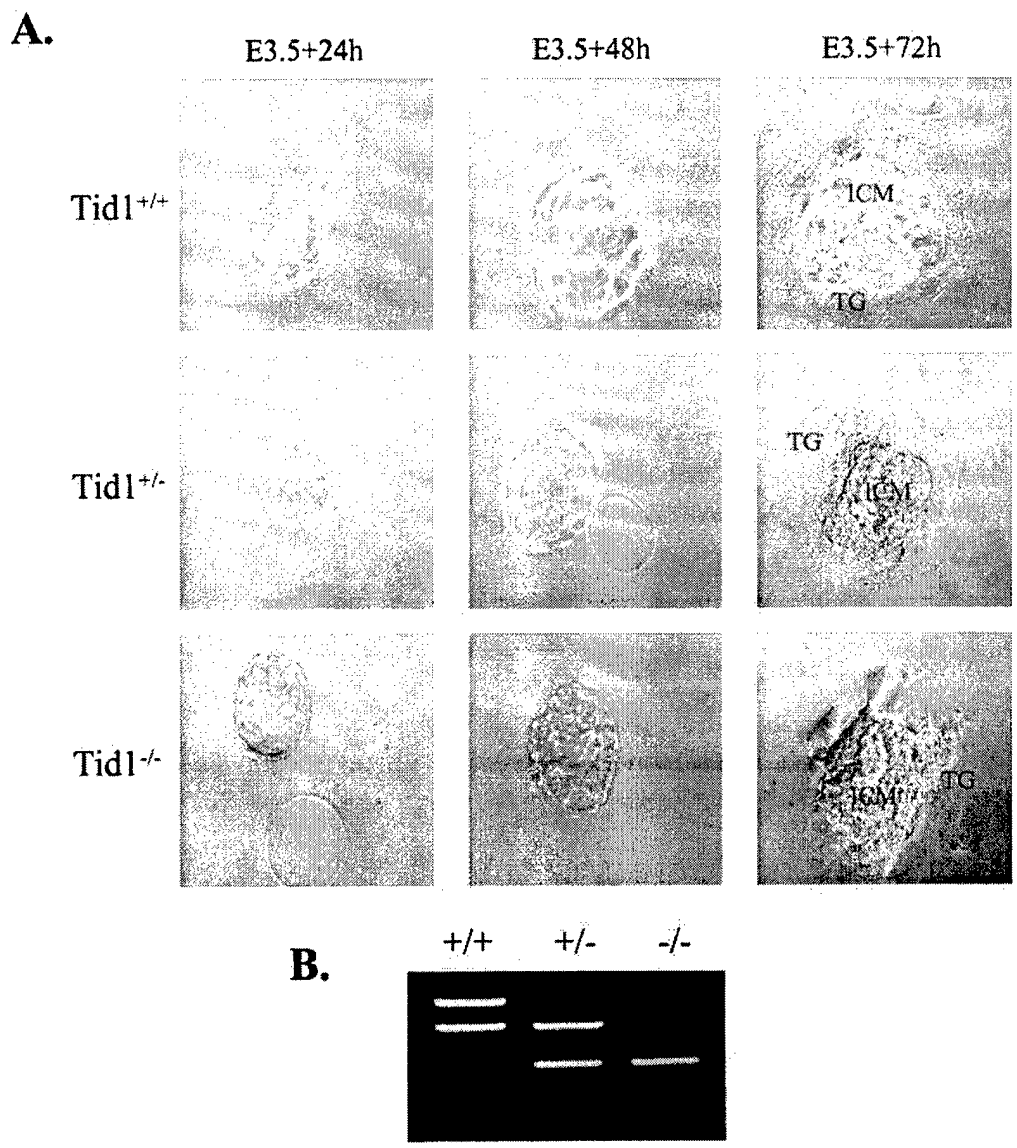

FIG. 2. *Tid1*$^{-/-}$ blastocysts were viable, hatched, and formed an inner cell mass and trophectoderm. (A) Blastocysts derived from *Tid1*$^{+/-}$ intercrosses were cultured in vitro for 3 days. In each outgrowth, the inner cell mass (ICM) and trophectoderm showed no differences. TG, trophoblast giant cell. (B) The genotype of each outgrowth was determined by PCR as described in the legend to Fig. 1D. The patterns of electrophoresed nested-PCR products are shown for ES cells with *Tid1*$^{+/+}$, *Tid1*$^{+/-}$, and *Tid1*$^{-/-}$ genotypes.

centrifugation in CsCl. High-titer stocks contained 1×10^{12} to 10×10^{12} virus particles/ml, determined by using bovine serum albumin as a standard, with 1 μg of viral protein considered to be 4×10^9 virus particles. For adenovirus infection of MEFs, a multiplicity of infection of 5×10^4 was used to reach a 100% infection rate.

Immunofluorescence. MEFs were seeded into 12-well plates containing collagen-coated glass coverslips and allowed to adhere overnight. The slides were washed with PBS and fixed in 4% paraformaldehyde in PBS for 30 min at room temperature. After three washes with PBS, the cells were permeabilized with 0.5% Triton X-100 in PBS for 10 min at room temperature, rinsed, and blocked in 10% normal goat serum (Vector Laboratories, Burlingame, Calif.) for 1 h at room temperature. Next, the slides were incubated with 10 μg of affinity-purified murine Tid1 antibody in 2% goat serum/ml for 1 h at room temperature. Subsequently, the cells were incubated for 30 min with biotinylated goat anti-rabbit IgG (Vector Laboratories), rinsed, and incubated with streptavidin (1:1,000 dilution) conjugated with Alexa Fluor 568 (Molecular Probes Inc.) for 30 min at room temperature. Free streptavidin and biotin were blocked by using the avidin/biotin blocking kit (Vector Laboratories). Slides were incubated with 5 mg of the anti-mtHsp70 monoclonal antibody (Affinity Bioreagents, Golden, Colo.)/ml for 1 h, rinsed, and incubated with Alexa Fluor 488-conjugated goat anti-mouse IgG (Molecular Probes Inc.) for 30 min. The nuclei of cells were stained with 2 μM ToPro 3 staining dye (Molecular Probes Inc.) for 20 min. The cells were viewed and photographed with the Bio-Rad MRC1024 laser scanning confocal microscope attached to a Zeiss Axiovert S100TV microscope. Images were collected on the confocal microscope using Bio-Rad's LaserSharp (version 3.2) software. For mitochondrial staining, live cells adhering to coverslips were fed with 0.5 μM Mitotracker Green FM (Molecular Probes Inc.) in fresh medium for 30 min at 37°C. Subsequently, the cells were fixed and permeabilized as described above. The cells were stained with anti-apoptosis-inducing factor (AIF), anti-cytochrome *c* (Santa Cruz Biotechnology), anti-Tid1, or anti-mtHsp70, respectively.

cDNA microarray. cDNA microarrays containing ~13,000 mouse cDNA clones in three physically different slides were used. The cDNA clones were obtained commercially from Research Genetics (IMAGE consortium) and Incyte Genomics, as well as internal sources. Each clone was printed as two

independent spots on a given chip, on the left and right sides. Printing, hybridization, scanning, and image analysis have been previously described (2).

Statistical analysis of microarray data. From $Tid1^{f/+}$ and $Tid1^{f/-}$ MEFs on days 4, 5, and 6 after Ad-Cre treatment, total RNAs were collected and hybridized to cDNA microarrays. Intensity data were multiplicatively normalized to the 75th percentile of each microarray, which was arbitrarily set to the value of 100. The normalized data were analyzed by the *t* test comparing the $Tid1^{f/+}$ and $Tid1^{f/-}$ MEFs on days 4, 5, and 6. The normalized data were also analyzed by using the analysis of variance model, considering that day {4, 5, or 6} and type {$Tid1^{f/+}$ and $Tid1^{f/-}$ MEFs} are two factors with interaction. By using this model, *P* values were generated for each gene on the microarray for the effects of day, type, and day-and-type interaction. Ratios were calculated by using median values for each group. The *P* value of 0.05 was used as the cutoff for selecting genes with significant changes.

Reverse transcription-PCR (RT-PCR). Total RNAs were isolated from $Tid1^{f/+}$ and $Tid1^{f/-}$ MEFs on day 6 after the Ad-Cre treatment. First-strand cDNAs were synthesized from these RNAs (1 μg) with the SuperScript Preamplification system kit (Invitrogen, Carlsbad, Calif.). First-strand cDNA (0.1 μg) was then used for PCR with specific oligonucleotide primers designed for detecting messages of BAG1, MEK7, or GAPDH (glyceraldehyde-3-phosphate dehydrogenase). The individual primer sets for GAPDH, BAG1, and MEK7 were as follows: GAPDH sense (5′-TGCACCACCAACTGCTTAGC-3′) and antisense (5′-GGCATGGACTGTGGTCATGAG-3′); BAG1 sense (5′-CGTG ATCGTCACCCACAGCAA-3′) and antisense (5′-CAACAAGCTGAGCCAA GTCTT-3′); and MEK7 sense (5′-CGCATCGACCCTCCAGATCC-3′) and antisense (5′-CTGTCCTGTTGCCAGCTCCAC-3′). The numbers of PCR cycles for amplifying specific gene products were 26 (*BAG1*), 28 (*MEK7*), and 22 (*GAPDH*). The PCR products were separated by electrophoresis through 4% agarose and visualized by ethidium bromide staining.

RESULTS

Generation of *Tid1* floxed and mutant mice. To determine the pathophysiological function of *Tid1* both during early development and in adults, we used a conditional knockout strategy to generate mouse ES cell lines with a mutant *Tid1* allele. Briefly, a targeting vector was constructed by inserting two loxP sequences flanking exon 2 of the *Tid1* gene (Fig. 1A and B). A Cre-mediated excision of this *Tid1* floxed allele deleted exon 2 of the *Tid1* gene and also created a frameshift, disrupting the translation of the key functional domains of Tid1, including the DnaJ domain, a glycine- and phenylalanine (G/F)-rich region, a cysteine-rich part resembling a zinc finger and consisting of four CXXCXGXG repeats, and a nonhomologous C-terminal domain (24). Therefore, deleting exon 2 of *Tid1* would most likely lead to a null phenotype. We produced the *Tid1* floxed mice, which developed to adulthood normally and appeared to be healthy for at least 12 months after birth.

Loss of Tid1 resulted in embryonic lethality between E4.5 and E7.5, but $Tid1^{-/-}$ blastocysts are viable. Deletion of the *Tid1* gene in all tissues was achieved by crossing $Tid1^{+/targeted}$ mice with a general deletor mouse strain [FVB/N-TgN(ACTB-Cre)] carrying the *ACTB-Cre* gene (Fig. 1C and D), and the offspring of this cross that had the $Tid1^{+/-}$ genotype were later intercrossed. The resultant 121 weaned pups were genotyped, and no $Tid1^{-/-}$ mice were found, indicating that animals lacking functional *Tid1* are not viable. Heterozygous mutant and wild-type mice were born at an ~2:1 ratio (Table 1) and grew normally with no discernible phenotypic differences for >9 months.

To determine the stage of embryonic development at which the homozygous mutant embryos die, we isolated and genotyped embryos at E7.5, E8.5, E9.5, E10.5, E12.5, and E13.5 from heterozygote ($Tid1^{+/-}$) intercrosses (Table 1). For each time point analyzed, no homozygous mutant embryos were recovered, suggesting that $Tid1^{-/-}$ embryos die before E7.5 ($P < 0.01$) (Table 1). The ratio between heterozygous and wild-type embryos is 2:1. Approximately 25% of the total implantation sites were empty, suggesting that implantation had occurred at these sites but failed to proceed beyond E7.5 (Table 1). Conceivably, the $Tid1^{-/-}$ embryos were responsible for these empty sites; if so, *Tid1* null embryos could implant (E4.5) but were unable to survive in the uterus through E7.5.

The failure of $Tid1^{-/-}$ embryos to develop past E7.5 suggested that at the early development phase *Tid1* might be required for blastocyst formation. The E3.5 embryos from heterozygote intercrosses were isolated and allowed to develop for up to 3 days in vitro on gelatinized petri dishes (Fig. 2A). After that, viable blastocysts were genotyped (Fig. 2B). Eighteen percent (9 of 49) of these were homozygous mutants, 53% (26 of 49) were heterozygotes, and 29% (14 of 49) were wild type, which agrees with the Mendelian ratio of 1:2:1 (Table 1). Mutant blastocysts formed an inner cell mass and trophectoderm and were morphologically indistinguishable from wild-type and heterozygote outgrowths (Fig. 2A). These results suggest that *Tid1* is not required for blastocyst establishment but is required for later embryonic development between E4.5 and E7.5.

Tid1 is critical for embryonic-fibroblast survival. To explore the reason for the early death of Tid1-deficient embryos, we established MEFs with the genotypes $Tid1^{+/+}$, $Tid1^{+/-}$, $Tid1^{f/f}$, $Tid1^{f/+}$, and $Tid1^{f/-}$. Treating these MEFs with recombinant adenovirus encoding Cre recombinase effectively and irreversibly disrupted the *Tid1* floxed allele and abrogated consequent Tid1 protein production from the *Tid1* floxed allele. As shown

FIG. 3. *Tid1* gene product is required for cell survival. (A) MEFs with $Tid1^{+/+}$, $Tid1^{+/-}$, $Tid1^{f/+}$, $Tid1^{f/-}$, and $Tid1^{f/f}$ genotypes were infected with Ad-Cre (Cre) (+) or uninfected (−) as indicated. After 6 days, total cellular proteins from these cells were collected and separated by SDS-polyacrylamide gel electrophoresis and analyzed by Western blotting with an antibody against mouse Tid1. The recombinant Tid1L and Tid1S proteins generated from 293T cells transfected with expression plasmids encoding Tid1-L or Tid1-S (two splicing isoforms of Tid1) were used as controls. u.p., unprocessed; p., processed; n.s., nonspecific. (B) After infection with nothing (Mock), control adenovirus (control), or Ad-Cre (Cre) as indicated, the above-mentioned MEF cell lines were analyzed for growth and viability by MTT (3-[4,5-dimethylthiazol-2-yl]-2,5-diphenyltetrazolium bromide) assays at the indicated time intervals. OD560, optical density at 560 nm. The error bars indicate standard deviations. (C) $Tid1^{f/+}$ and $Tid1^{f/-}$ MEFs were treated as for panel A. After 9 days, genomic DNAs were purified from these cells and separated by agarose gel electrophoresis (top). Some MEFs were also treated with 50 μM zVAD (a caspase 3 inhibitor) as indicated. The relative amounts of viable cells for these treated MEFs were also assessed by MTT assays (bottom). (D) $Tid1^{f/+}$ and $Tid1^{f/-}$ MEFs were treated with 5 μg of anisomycin/ml (50 μM zVAD) as indicated for 18 h, and their genomic DNAs (top) and viabilities (bottom) were analyzed as for panel C. The MTT assays were performed in triplicate and repeated at least three times (the values are means plus standard deviations). (E) $Tid1^{f/+}$ and $Tid1^{f/-}$ MEFs were infected with Ad-Cre and collected at the indicated time intervals. The cells were fixed and stained with propidium iodide (PI) and analyzed by flow cytometry.

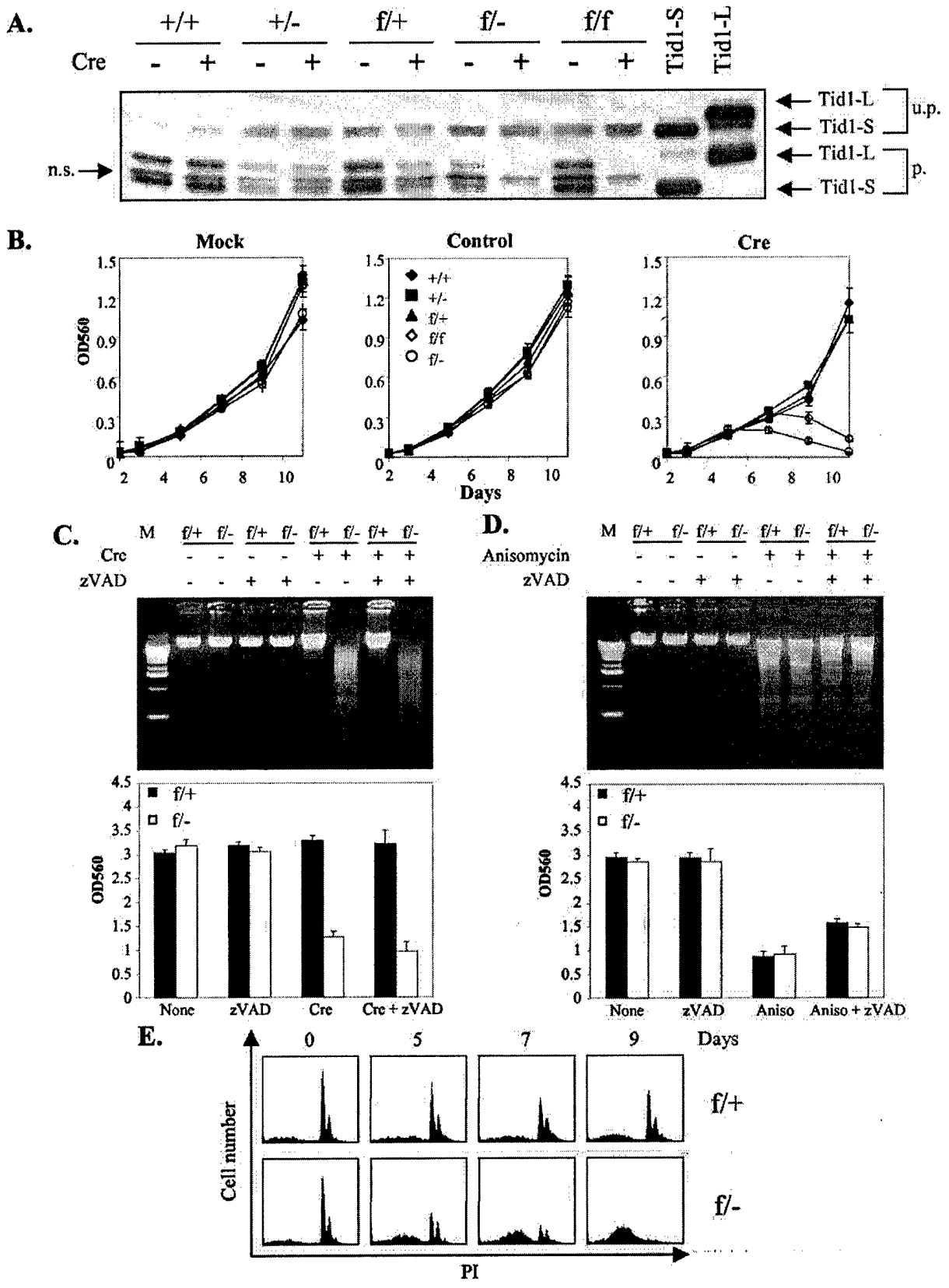

FIG. 3—*Continued.*

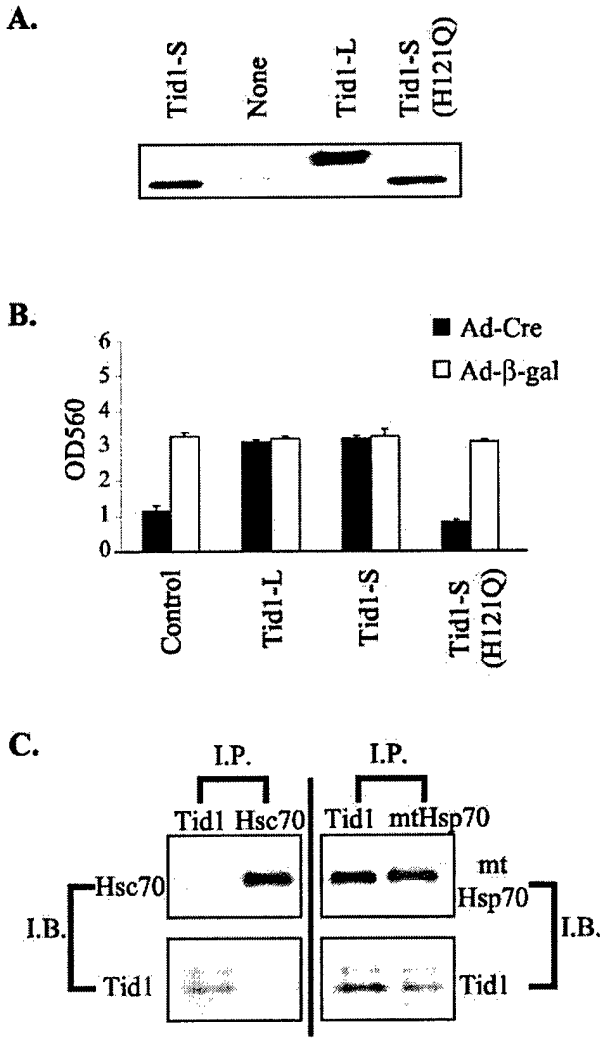

FIG. 4. DnaJ domain-dependent interaction between Tid1 and Hsp70 is critical for cell survival. (A) Total proteins were collected from $Tid1^{f/-}$ MEFs infected with recombinant adenoviruses encoding human Tid1-L, Tid1-S, or Tid1-S (H121Q) as indicated and analyzed by Western blotting with the anti-Tid1 antibody. (B) $Tid1^{f/-}$ MEFs were first infected with Ad-Cre or Ad-β-gal adenovirus, and after 2 days, the treated cells were infected with adenoviruses encoding human Tid1-L, Tid1-S, or Tid1-S (H121Q) as indicated. Nine days after the first infection, the number of viable cells for these MEFs was determined by MTT assay. OD560, optical density at 560 nm. The error bars indicate standard deviations. (C) Endogenous Tid1-L and Tid1-S proteins coimmunoprecipitated with mtHsp70. Total protein from MEFs was used for immunoprecipitation (I.P.) experiments with antibody specific for Tid1, mtHsp70, or Hsc70. The resulting immunocomplexes were analyzed by immunoblotting (I.B.) with antibody against Tid1, mtHsp70, or Hsc70, as indicated.

in Fig. 3A, after Ad-Cre treatment, both splicing isoforms of Tid1 protein, Tid1-S and Tid1-L (22, 25), were completely removed in $Tid1^{f/-}$ and $Tid1^{f/f}$ MEFs, and the amount of Tid1 protein produced from $Tid1^{f/+}$ MEFs was about half the amount produced from $Tid1^{+/+}$ MEFs (Fig. 3A). The earliest stage that Tid1 proteins became undetectable was on day 4 after the Ad-Cre treatment in $Tid1^{f/-}$ and $Tid1^{f/f}$ MEFs (data not shown). The growth of treated MEFs was normal in cells with either one or both *Tid1* genes intact. On the other hand, the proliferation of Tid1-deficient MEFs was impaired, and the number of viable cells declined dramatically 5 to 6 days after Ad-Cre addition (Fig. 3B). Eventually, none of the Tid1-deficient MEFs survived the Ad-Cre treatment. For MEFs infected with the control adenovirus, no growth difference was observed for each MEF cell type (Fig. 3B).

To characterize further the acute cell death triggered by *Tid1* deletion, we subjected $Tid1^{f/-}$ and $Tid1^{f/+}$ MEFs, after disruption of the *Tid1* floxed allele, to DNA fragmentation and fluorescence-activated cell sorter analysis (Fig. 3C and E). The genomic DNA from Ad-Cre-treated $Tid1^{f/-}$ cells showed DNA degradation in the form of DNA smearing rather than DNA laddering (Fig. 3C). Fluorescence-activated cell sorter analysis also showed that with Ad-Cre infection, the $Tid1^{f/-}$ MEFs increased their subdiploid DNA contents (Fig. 3E). Both the DNA smearing and the increase in subdiploid DNA suggest that the Tid1-deficient MEFs were undergoing a process of cell death that is not typical apoptosis (Fig. 3C and E). On the other hand, the growth and viability of $Tid1^{f/+}$ MEFs after Ad-Cre infection, with one *Tid1* allele remaining intact, were not affected (Fig. 3B, C, and E). Moreover, in the presence of the caspase 3 inhibitor zVAD, the death of Tid1-deficient cells was not reduced (Fig. 3C), and the cell death triggered by the apoptosis inducer aniosmycin was partially blocked in both $Tid1^{f/+}$ and $Tid1^{f/-}$ cells (Fig. 3D). These results suggest that cell death caused by *Tid1* removal is not mediated by a typical caspase 3-dependent apoptotic process.

A functional DnaJ domain of Tid1 is essential for viability of MEF cells. As a DnaJ protein family member, Tid1 interacts with Hsp70 proteins via its highly conserved DnaJ domain and subsequently activates the ATPase activity of Hsp70. To test whether the J domain in Tid1 was critical for the role of Tid1 in cell survival, we generated a Tid1 protein with an impaired J domain, Tid1-S(H121Q), by mutating one amino acid residue within the J domain that is critical for the interaction of Tid1 with Hsp 70 proteins (Fig. 4A) (25). Ad-Cre-treated $Tid1^{f/-}$ cells subsequently infected with adenovirus encoding either wild-type Tid1-S or Tid1-L could survive the loss of the functional *Tid1* allele (Fig. 4B). In contrast, infection with Ad-Tid1-S(H121Q) adenovirus failed to compensate for the disruption of the normal *Tid1* gene within $Tid1^{f/-}$ MEFs (Fig. 4B). These data suggest that Tid1 association with Hsp70 is critical for maintaining the survival of MEFs.

The Tid1 protein has been shown to interact with both mitochondrial heat shock protein 70 (mtHsp70) and nonmitochondrial Hsp70 (25, 27). Nonetheless, Syken et al. (25) reported that in human osteosarcoma cells, U2OS, the Tid1 protein interacts only with mtHsp70 and not with cytosolic Hsp70 (Hsc70). To identify which Hsp70 Tid1 interacts with in

FIG. 5. Tid1 and mtHsp70 proteins colocalize within mitochondria. (A) Immunofluorescence staining of Tid1 and mtHsp70 proteins in $Tid1^{f/+}$ and $Tid1^{f/-}$ MEFs 5 days after treatment with Ad-Cre. (B) The same Ad-Cre-treated $Tid1^{f/+}$ and $Tid1^{f/-}$ MEFs were first stained with Mitotracker and subsequently double stained with antibody against Tid1, mtHsp70, cytochrome *c* (Cyto. C), or AIF as indicated.

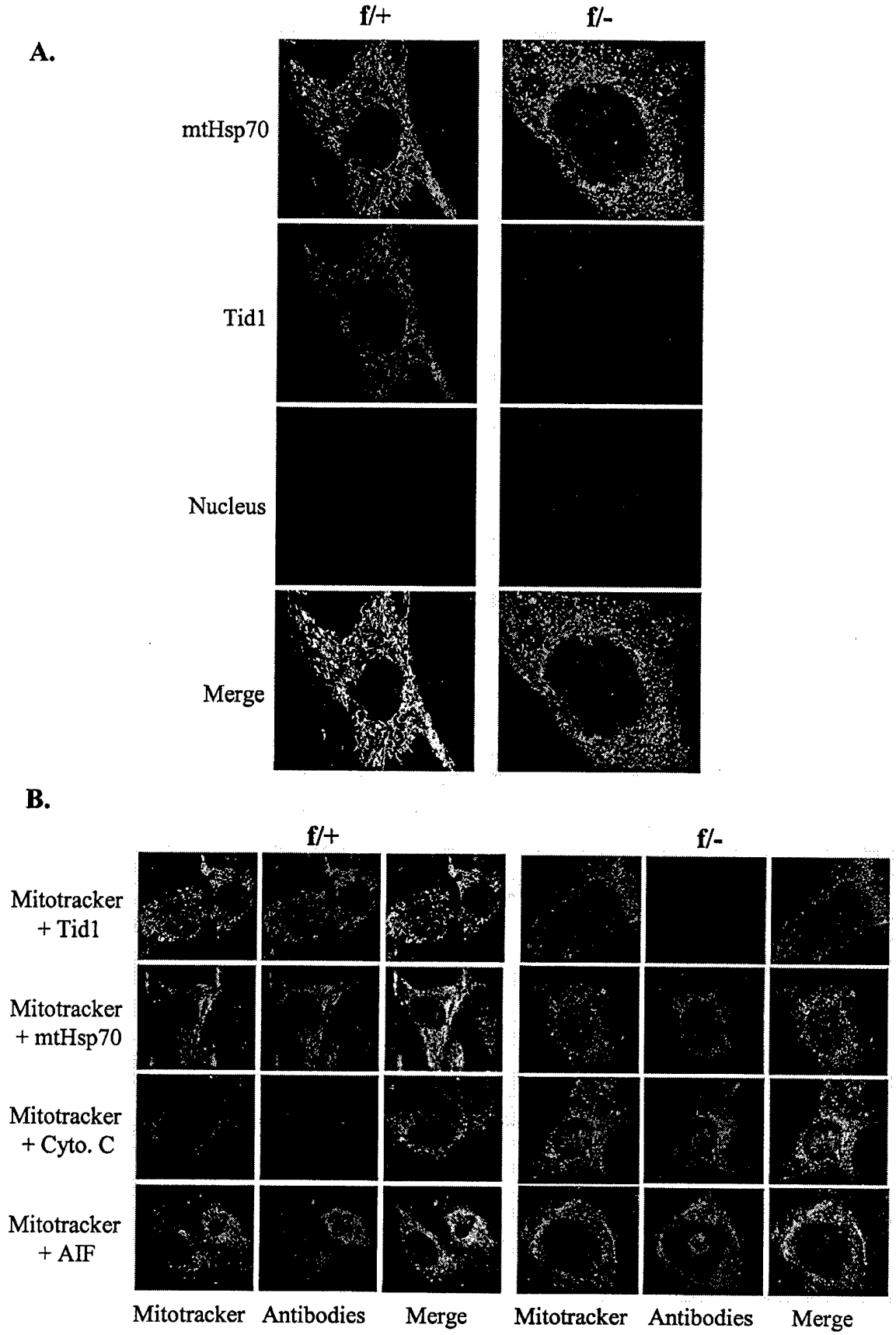

FIG. 5—*Continued.*

MEFs, we used specific antibody against Tid1, mtHsp70, or the nonmitochondrial Hsp70 homolog, Hsc70, in coimmunoprecipitation-immunoblotting experiments. The antibody specific for mouse Tid1 immunoprecipitated both mature forms of Tid1 associated with mtHsp70 but did not immunoprecipitate Hsc70 from MEFs (Fig. 4C). The antibody specific for mtHsp70 protein immunoprecipitated mtHsp70 in complex with Tid1, but in immunoprecipitates prepared from cell extracts with the anti-Hsc70 antibody, no Tid1 was detected (Fig. 4C).

We further investigated the subcellular localization of Tid1 in MEFs by immunofluorescence microscopy. In *Tid1*$^{f/+}$ MEFs, 5 days after Ad-Cre infection, endogenous Tid1 and mtHsp70 were separately stained by using antibody specific for either Tid1 or mtHsp70. Both Tid1 and mtHsp70 were detected mostly in the cytoplasm, colocalized, and displayed a short filamentous pattern (Fig. 5A). Not surprisingly, no Tid1 protein could be detected in Ad-Cre-treated *Tid1*$^{f/-}$ MEFs, and interestingly, the subcellular distribution of mtHsp70 turned punctate (Fig. 5A). The change of the subcellular distribution of mtHsp70 from short filament to punctate was not dependent on the genotype of the MEFs, since before the deletion of *Tid1*, mtHsp70 and Tid1 colocalized in a short-string pattern within the cytosol of *Tid1*$^{f/-}$ MEFs (data not shown). These data suggest that the Tid1 protein in MEFs is located within the cytoplasm and that mtHsp70 is the major Hsp70 in complex with Tid1. To further examine the subcellular localization of Tid1 or mtHsp70 in MEFs, Mitotracker, a mitochondrion-specific dye, was used. In *Tid1*$^{f/+}$ MEFs 5 days after Ad-Cre infection, most of the Tid1 costained with the Mitotracker, demonstrating that Tid1 proteins were mainly restricted within the mitochondria (Fig. 5B).

Similar patterns were observed when *Tid1*$^{f/+}$ MEFs were double-stained with Mitotracker and mtHsp70, Mitotracker and cytochrome *c*, or Mitotracker and AIF (Fig. 5B). In Ad-Cre-treated *Tid1*$^{f/-}$ MEFs, the intensity of Mitotracker staining was attenuated compared to that of *Tid1*$^{f/+}$ MEFs (Fig. 5B). Interestingly, some AIF proteins were translocated from the mitochondria to the nucleus, suggesting that the *Tid1*$^{f/-}$ MEFs, with Tid1 deleted, were undergoing the process of cell death (Fig. 5B).

Decreased expression of *BAG1* and *MEK7* genes is partially responsible for cell death resulting from Tid1 removal. The role of Tid1 in sustaining cell survival most likely occurs through its association with mtHsp70 and the consequent biological effect of this interaction. It has been demonstrated that mitochondrial Hsp70 (mtHsp70/mortalin/Grp75) influences cell mortality by modulating the p53-mediated gene expression of two downstream proteins, MDM2 and p21 (30). Thus, the impact on the expression levels of the p53, MDM2, and p21 proteins was assessed after *Tid1* removal in MEFs. We detected no significant alteration in the expression of these proteins (data not shown). Next, by cDNA microarray, we examined 13,000 known genes to determine the gene expression profiles altered by *Tid1* removal. Total RNAs from both Ad-Cre-infected *Tid1*$^{f/+}$ and *Tid1*$^{f/-}$ MEFs were purified and examined by cDNA microarray-based analysis. After statistical analysis, we found a total of 91 genes that showed a >2-fold change caused by disrupting both Tid1 alleles (data not shown). Among these, we found that the expression of the BAG1 and MEK7 genes, important for cell growth and survival (8, 26), decreased >2.5-fold in cells without the Tid1 protein. Semiquantitative RT-PCR analysis was used to confirm the results from the cDNA microarray (Fig. 6A). Additionally, by immunoblot assay, the decreased expression of BAG1 and MEK7 proteins after *Tid1* deletion was established by comparing their expression levels in *Tid1*$^{f/+}$ and *Tid1*$^{f/-}$ MEFs after Ad-Cre treatment. The expression of the internal control, β-actin, was not altered in these two treated MEFs (Fig. 6B). For determining the contribution of BAG1 and MEK7 in Tid1-dependent cell survival, adenoviruses expressing human recombinant BAG1 or MEK7 were constructed and introduced, separately or jointly, into *Tid1*$^{f/-}$ MEFs 2 days after the infection of Ad-Cre. Supplementary MEK7 or BAG1 prevented 12 or 31%, respectively, of cell death caused by the loss of *Tid1* in *Tid1*$^{f/-}$ cells (Fig. 6C). Combined treatment with Ad-MEK7 and Ad-BAG1 had an additive effect on rescuing cell death in *Tid1*$^{f/-}$ cells with Tid1 deleted, suggesting that the survival signals generated from MEK7 or BAG1 do not overlap in Tid1-deficient MEFs. These results indicate that the decreased expression of BAG1 and MEK7 partially accounts for the cell death induced by removing endogenous Tid1 protein from MEFs.

DISCUSSION

In this study, we generated a null mutation of the *Tid1* gene by homologous recombination in mouse ES cells. The *Tid1* mutation does not affect the differentiation of the diploid trophoblast in the inner cell mass tissue of the early embryonic blastocyst and yet was lethal before E7.5 of gestation. Interestingly, no hyperproliferative phenotype was observed in the Tid1-null embryos of mice, as was observed in the Tid 56 mutant embryo of *Drosophila* (16). This phenotypic divergence between mammal and insect might be caused by a developmental role of *Tid1* in mammals different from that of its *Drosophila* counterpart, *Tid56*. However, we cannot exclude the possibility that in mammals a protection mechanism exists that aborts embryogenesis once the *Tid1* mutant embryo becomes tumorigenic. If this is the case, the window to identify those embryos would be very small (between E4.5 and E7.5), and within that period of time, the embryos would be too tiny to isolate and to genotype. The other possibility is that *Tid1* is vital for certain crucial cell types during early embryonic development and that disruption of the *Tid1* gene in these cells causes embryonic lethality, preventing the observation of the anticancer function of *Tid1* for other cell types generated in the later stages of embryogenesis and/or in the adult animal. Early lethality has also been observed in mouse embryos deficient in other tumor suppressors, such as *Brca1*, *Brca2*, and *Rb*, due to their roles in cellular proliferation and differentiation during early development (11, 12, 19, 31). Therefore, it is not unexpected that Tid1, as a putative tumor suppressor, has a role in embryonic development.

Tid1 binds to mtHsp70/mortalin, whose function has been suggested in orchestrating protein transfer across mitochondrial membranes, as well as in cell survival, for its inhibitory effect on p53 (30). However, *Tid1* deletion in MEFs does not affect p53-dependent transcription of MDM2 and p21. Possibly, the Tid1/mtHsp70 complex is not involved in modulating

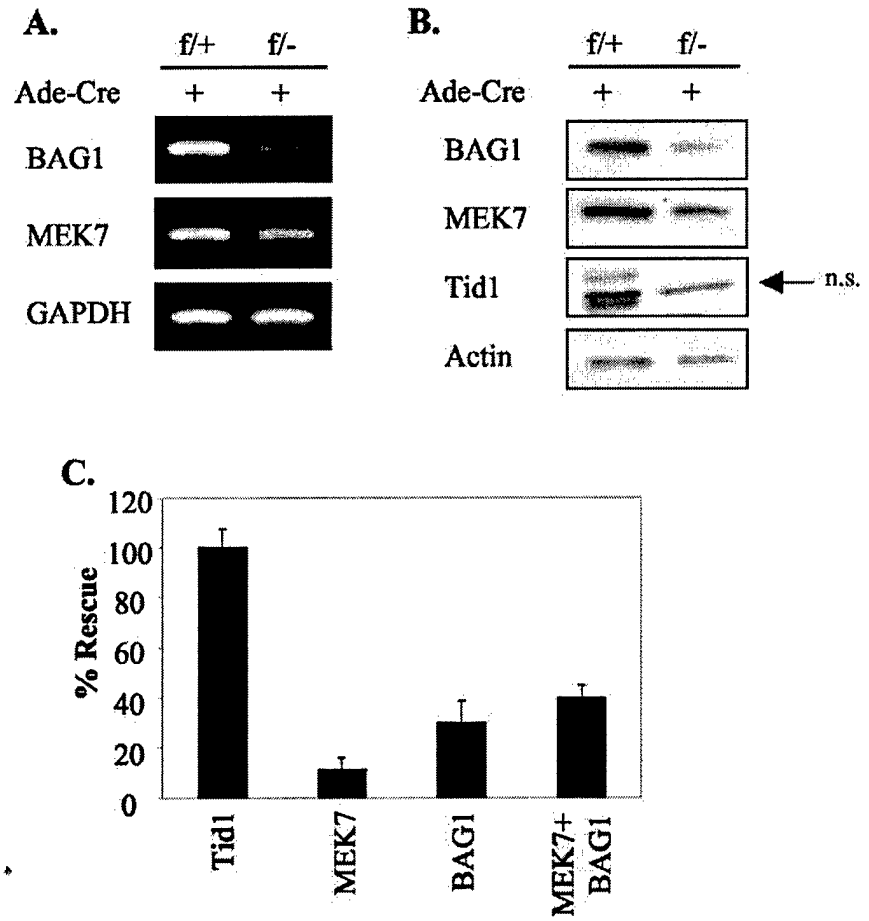

FIG. 6. Decreased expression of *BAG1* and *MEK7* genes is partially responsible for cell death resulting from cellular Tid1 removal. (A) $Tid1^{f/+}$ and $Tid1^{f/-}$ MEFs were infected (+) with Ad-Cre, and after 6 days, total RNAs from these MEFs were collected and analyzed by semiquantitative RT-PCR with the specific primer set for *BAG1*, *MEK7*, or *GAPDH*. The PCR products were separated through 4% agarose. (B) Total cellular extracts were prepared from these Ad-Cre-treated $Tid1^{f/+}$ and $Tid1^{f/-}$ cells and analyzed by immunoblotting with anti-Tid1, anti-BAG1, anti-MEK7, or anti β-actin antibodies as indicated. n.s., nonspecific. (C) $Tid1^{f/-}$ MEFs were infected with Ad-Cre on day 1 and infected with human recombinant Tid1, BAG1, or MEK7 adenovirus on day 3. The number of viable cells on day 9 for each treated cell type was measured by MTT assay. The rescue rate for cells treated with the combination of Ad-Cre and Ad-Tid1 was set as 100%, and 0% was set for cells treated with Ad-Cre only. The error bars indicate standard deviations.

p53 activity, at least during early embryogenesis or in embryonic fibroblasts. Nevertheless, we found that *Tid1* removal significantly reduces transcription and consequently lowers the level of protein expression of two molecules, BAG1 and MEK7, whose functions in sustaining cell survival have been demonstrated (8, 26). BAG1 is a multifunctional protein that has affinity with a wide variety of cellular targets for regulating cell survival pathways, and its expression is frequently altered in malignant cells (26). MEK7 is one of the MAP2K proteins of the signal pathway of c-Jun N-terminal protein kinase (JNK), which is a critical mediator for transducing message from activated MAP3K to MAPK (JNK) (8). The JNK signaling pathway is critical in regulating both the apoptotic and the antiapoptotic processes (8); thus, it is logical that down-regulation of MEK7 expression is partially responsible for the death of Tid1-deficient MEFs. Tid1 has also been shown to interact with RasGAP and Jak2 kinase to regulate growth control pathways (21, 27), possibly through its role as a co-chaperone for Hsp70 (21, 27). These pathways are both important for delivering antiapoptotic or growth signals, resulting in hyperproliferation and, sometimes, cancerous cellular phenotypes (4, 29). Key downstream effectors for these pathways are transcriptional machineries which, after activation, augment the expression of mitogenic genes (4, 29). It will be interesting to see whether the transcription of the *BAG1* and *MEK7* genes is affected by these two signaling pathways in a Tid1-dependent manner.

More than two dozen tumor suppressor genes are known in *Drosophila* (9, 10). A number of these genes have human homologues whose tumor suppressor functions have been well documented, such as PTEN, RB, and $p16^{INK4a}$ (3, 20, 23). The anticancer roles of the mammalian counterparts of some of these fly tumor suppressor genes, such as that of Tid56 (Tid1), are not clear, although the loss of Tid1 expression has been implicated in basal cell carcinoma (5). Several reports have associated the functions of Tid1 in processing oncoproteins, for modulating transformation signals, and in regulating apoptotic and antiapoptotic signaling pathways (6, 7, 21, 22, 27). Addi-

tionally, overexpression of Tid1 reduces the uncontrolled growth of cancer cells (7). Decreasing cellular Tid1 should promote the proliferation or the malignancy of cells, but we see an opposite effect in embryonic fibroblasts (Fig. 3B). One possible reason is that Tid1 has different functions in different cell types or at different stages of development. This hypothesis is supported by our recent observation that mice with a hepatocyte-specific *Tid1* deletion are viable and appear healthy at 4 weeks of age (unpublished data). The other possibility is that loss of *Tid1* might lead to an epigenetic condition that results in cell death, excluding those rare cells that undergo additional mutations and develop into cancer. A precedent in carcinogenesis for this kind of inconsistency is the discovery of c-*myc*: in primary cells, overexpression of c-*myc* leads to programmed cell death (15); however, for rare cells that contain additional mutations, such as in *bcl2*, *bax*, or *ras*, elevated c-*myc* promotes their proliferation and survival and induces them to malignancy (1, 13).

To study the pathophysiological function of *Tid1* in adult animals and to investigate the role that the loss of this (potential) tumor suppressor gene plays in tumor initiation and progression in vivo, we will take advantage of the conditional nature of *Tid1* floxed mice to circumvent the early embryonic death caused by global deletion of *Tid1*. We are currently breeding our conditional knockout model with various Cre transgenic lines to generate mice in which deletion of the *Tid1* gene is restricted to certain types of tissues or selected cell lineages, as well as generating mice in which removal of the Tid1 protein is inducible in adult animals.

In summary, our results demonstrate that Tid1 is a crucial element in early embryogenesis and for sustaining embryonic-cell survival. We also provide evidence that the generation of Tid1-dependent survival signals requires interaction between Tid1 and the Hsp70 chaperone.

REFERENCES

1. **Aunoble, B., R. Sanches, E. Didier, and Y. J. Bignon.** 2000. Major oncogenes and tumor suppressor genes involved in epithelial ovarian cancer. Int. J. Oncol. **16**:567–576.
2. **Bonaventure, P., H. Guo, B. Tian, X. Liu, A. Bittner, B. Roland, R. Salunga, X. J. Ma, F. Kamme, B. Meurers, et al.** 2002. Nuclei and subnuclei gene expression profiling in mammalian brain. Brain Res. **943**:38–47.
3. **Bosco, G., W. Du, and T. L. Orr-Weaver.** 2001. DNA replication control through interaction of E2F-RB and the origin recognition complex. Nat. Cell Biol. **3**:289–295.
4. **Campbell, S. L., R. Khosravi-Far, K. L. Rossman, G. J. Clark, and C. J. Der.** 1998. Increasing complexity of Ras signaling. Oncogene **17**:1395–1413.
5. **Canamasas, I., A. Debes, P. G. Natali, and U. Kurzik-Dumke.** 2003. Understanding human cancer using drosophila: Tid47, a cytosolic product of the DnaJ-like tumor suppressor gene l(2)tid, is a novel molecular partner of patched related to skin cancer. J. Biol. Chem. **278**:30952–30960.
6. **Cheng, H., C. Cenciarelli, M. Tao, W. P. Parks, and C. Cheng-Mayer.** 2002. HTLV-1 Tax-associated hTid-1, a human DnaJ protein, is a repressor of IκB kinase beta subunit. J. Biol. Chem. **277**:20605–20610.
7. **Cheng, H., C. Cenciarelli, Z. Shao, M. Vidal, W. P. Parks, M. Pagano, and C. Cheng-Mayer.** 2001. Human T cell leukemia virus type 1 Tax associates with a molecular chaperone complex containing hTid-1 and Hsp70. Curr. Biol. **11**:1771–1775.
8. **Dhanasekaran, N., and R. E. Premkumar.** 1998. Signaling by dual specificity kinases. Oncogene **17**:1447–1455.
9. **Gateff, E.** 1994. Tumor suppressor and overgrowth suppressor genes of *Drosophila melanogaster*: developmental aspects. Int. J. Dev. Biol. **38**:565–590.
10. **Gateff, E., and B. M. Mechler.** 1989. Tumor-suppressor genes of *Drosophila melanogaster*. Crit Rev. Oncog. **1**:221–245.
11. **Gowen, L. C., B. L. Johnson, A. M. Latour, K. K. Sulik, and B. H. Koller.** 1996. Brca1 deficiency results in early embryonic lethality characterized by neuroepithelial abnormalities. Nat. Genet. **12**:191–194.
12. **Hakem, R., J. L. de la Pompa, C. Sirard, R. Mo, M. Woo, A. Hakem, A. Wakeham, J. Potter, A. Reitmair, F. Billia, E. Firpo, C. C. Hui, J. Roberts, J. Rossant, and T. W. Mak.** 1996. The tumor suppressor gene Brca1 is required for embryonic cellular proliferation in the mouse. Cell **85**:1009–1023.
13. **Hoffman, B., A. Amanullah, M. Shafarenko, and D. A. Liebermann.** 2002. The proto-oncogene c-myc in hematopoietic development and leukemogenesis. Oncogene **21**:3414–3421.
14. **Hogan, B., F. Costantini, R. Beddington, and E. Lacy.** 1995. Manipulating the mouse embryo: a laboratory manual, 2nd ed. Cold Spring Harbor Laboratory Press, Cold Spring Harbor, N.Y.
15. **Klefstrom, J., I. Vastrik, E. Saksela, J. Valle, M. Eilers, and K. Alitalo.** 1994. c-Myc induces cellular susceptibility to the cytotoxic action of TNF-alpha. EMBO J. **13**:5442–5450.
16. **Kurzik-Dumke, U., D. Gundacker, M. Renthrop, and E. Gateff.** 1995. Tumor suppression in *Drosophila* is causally related to the function of the lethal(2) tumorous imaginal discs gene, a *dnaJ* homolog. Dev. Genet. **16**:64–76.
17. **Kurzik-Dumke, U., A. Debes, M. Kaymer, and P. Dienes.** 1998. Mitochondrial localization and temporal expression of the *Drosophila melanogaster* DnaJ homologous tumor suppressor Tid50. Cell Stress Chaperones **3**:12–27.
18. **Li, B., J. C. Ruiz, and K. T. Chun.** 2002. CUL-4A is critical for early embryonic development. Mol. Cell. Biol. **22**:4997–5005.
19. **Ludwig, T., D. L. Chapman, V. E. Papaioannou, and A. Efstratiadis.** 1997. Targeted mutations of breast cancer susceptibility gene homologs in mice: lethal phenotypes of Brca1, Brca2, Brca1/Brca2, Brca1/p53, and Brca2/p53 nullizygous embryos. Genes Dev. **11**:1226–1241.
20. **Mayo, L. D., and D. B. Donner.** 2002. The PTEN, Mdm2, p53 tumor suppressor-oncoprotein network. Trends Biochem. Sci. **27**:462–467.
21. **Sarkar, S., B. P. Pollack, K. T. Lin, S. V. Kotenko, J. R. Cook, A. Lewis, and S. Pestka.** 2001. hTid-1, a human DnaJ protein, modulates the interferon signaling pathway. J. Biol. Chem. **276**:49034–49042.
22. **Schilling, B., T. De Medina, J. Syken, M. Vidal, and K. Munger.** 1998. A novel human DnaJ protein, hTid-1, a homolog of the *Drosophila* tumor suppressor protein Tid56, can interact with the human papillomavirus type 16 E7 oncoprotein. Virology **247**:74–85.
23. **Sherr, C. J.** 1996. Cancer cell cycles. Science **274**:1672–1677.
24. **Silver, P. A., and J. C. Way.** 1993. Eukaryotic DnaJ homologs and the specificity of Hsp70 activity. Cell **74**:5–6.
25. **Syken, J., T. De Medina, and K. Munger.** 1999. TID1, a human homolog of the *Drosophila* tumor suppressor l(2)tid, encodes two mitochondrial modulators of apoptosis with opposing functions. Proc. Natl. Acad. Sci. USA **96**:8499–8504.
26. **Takayama, S., and J. C. Reed.** 2001. Molecular chaperone targeting and regulation by BAG family proteins. Nat. Cell Biol. **3**:E237–E241.
27. **Trentin, G. A., X. Yin, S. Tahir, S. Lhotak, J. Farhang-Fallah, Y. Li, and M. Rozakis-Adcock.** 2001. A mouse homologue of the *Drosophila* tumor suppressor l(2)tid gene defines a novel Ras GTPase-activating protein (Ras-GAP)-binding protein. J. Biol. Chem. **276**:13087–13095.
28. **Tybulewicz, V. L., C. E. Crawford, P. K. Jackson, R. T. Bronson, and R. C. Mulligan.** 1991. Neonatal lethality and lymphopenia in mice with a homozygous disruption of the c-abl proto-oncogene. Cell **65**:1153–1163.
29. **Verma, A., S. Kambhampati, S. Parmar, and L. C. Platanias.** 2003. Jak family of kinases in cancer. Cancer Metastasis Rev. **22**:423–434.
30. **Wadhwa, R., S. Takano, M. Robert, A. Yoshida, H. Nomura, R. R. Reddel, Y. Mitsui, and S. C. Kaul.** 1998. Inactivation of tumor suppressor p53 by mot-2, a hsp70 family member. J. Biol. Chem. **273**:29586–29591.
31. **Williams, B. O., E. M. Schmitt, L. Remington, R. T. Bronson, D. M. Albert, R. A. Weinberg, and T. Jacks.** 1994. Extensive contribution of Rb-deficient cells to adult chimeric mice with limited histopathological consequences. EMBO J. **13**:4251–4259.